Geoderma Regional 44 (2026) e01066

Contents lists available at ScienceDirect

Geoderma Regional

journal homepage: www.elsevier.com/locate/geodrs

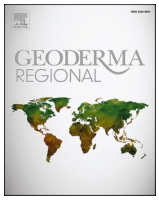

Soil fertility and maize response to subsoil deep tillage and termite mound amendments in strongly weathered plinthic soils

John Banza Mukalay [a,b,*], Jeroen Meersmans [a], Joost Wellens [a], Yannick Useni Sikuzani [c], Emery Kasongo Lenge Mukonzo [d], Gilles Colinet [a]

[a] Water-Soil-Plant Exchange Research Unit, TERRA Gembloux Agro-Bio-Tech, University of Liège, 5030 Gembloux, Belgium
[b] Department of Renewable Natural Resource Management, Faculty of Agricultural Sciences and Environment, University of Kolwezi, Kolwezi, P.O. Box 57, Democratic Republic of the Congo
[c] Ecologie, Restauration Écologique et Paysage, Faculté des Sciences Agronomiques, University of Lubumbashi, Lubumbashi, P.O. Box 1825, Democratic Republic of the Congo
[d] Land Evaluation, Soil Conservation and Agro-Meteorology Research Unit, Faculty of Agronomy, University of Lubumbashi, Lubumbashi, P.O. Box 1825, Democratic Republic of the Congo

ARTICLE INFO

Keywords:
Plinthite
Termite mounds
Subsoiling
Saturated hydraulic conductivity (Ksat)
Spline **w**ith **b**arriers
Lubumbashi

ABSTRACT

Plinthite, an iron-rich and humus-poor clay horizon that hardens irreversibly, poses major constraints to agriculture in the Lubumbashi region. Termite mound materials, which are enriched in basic cations, combined with subsoiling to fragment and remove plinthite, may improve soil fertility. This study evaluated the combined effects of subsoiling and termite mound amendments on Plinthosols under maize across ten blocks covering 660 ha. Surface soils (0–10 cm) were sampled, soil profiles were described, and maize yields were measured over two growing seasons. Spatial patterns of soil properties and yield were mapped using the Spline With Barriers method, and stepwise regression was applied to identify key variables controlling yield.

Soil thickness ranged from <9 cm in areas requiring secondary subsoiling to >73 cm in blocks B2, B5, B6, and B9. Soil pH (KCl) ranged from 4.1 to 7.8, while pH in water ranged from 4.9 to 8.7, with stronger acidity observed in blocks B8–B10. Total organic carbon (TOC) was generally low (0.4–2.5%). Nutrient contents were highly heterogeneous: P ranged from 5.1 to 145.5 mg kg^{-1}; Ca from 1360 to 18,268 mg kg^{-1}; K from 130.2 to 942.0 mg kg^{-1}; and Mg from 238.8 to 2987 mg kg^{-1}. Available Al (44–293 mg kg^{-1}), Fe (28.1–351.7 mg kg^{-1}), Mn (4.4–669 mg kg^{-1}) and Cu (1.9–25.8 mg kg^{-1}) also showed strong spatial variability. Bulk density decreased with depth, and although Ksat remained low, water retention was improved in the surface layer. Maize grain yield ranged from 2.3 to 11.1 t ha^{-1}, with seasonal means of 7.1–8.2 t ha^{-1}. Regression models identified soil pH, Ca, and TOC as the main positive determinants of maize yield, whereas high concentrations of Fe, Cu, and Mn were associated with reduced yields.

1. Introduction

In tropical Africa, soils are characterized by low intrinsic fertility, a condition largely driven by climatic and pedological constraints (Sanchez, **2018**). However, the economies of most tropical countries rely mainly on agriculture, a sector that must expand substantially to meet the pressures of rapid population growth and evolving market demands (Adeyanju et al., **2023**; Beyene, **2023**; Muhirwa et al., **2023**; Santos et al., **2023**). Recent statistics further indicate that nearly half of the African population faces moderate to severe food insecurity (FAO, **2021**; Gebre and Rahut, **2021**).

In the Democratic Republic of the Congo, and particularly in the Lubumbashi region, agricultural yields remain far below the genetic potential of crops, thereby contributing to food insecurity among a population that, according to Useni et al. (**2024**), exceeded 2.5 million inhabitants in 2020. Studies in this region show that soil degradation is a major constraint on agricultural productivity, due in large part to the prevalence of highly weathered soils with limited nutrient reserves (Banza et al., **2019**; Kasongo, **2008**; Kasongo et al., **2019**; Useni et al., **2014**), a situation also confirmed by the perception of local populations (N'tambwe Nghonda et al., **2023**). These soils typically display low chemical fertility (Camacho et al., **2021**; de Melo et al., **2020**; Koppe

* Corresponding author **at:** Water-Soil-Plant Exchange Research Unit, TERRA Gembloux Agro-Bio-Tech, University of Liège, 5030 Gembloux, Belgium.
E-mail address: john.banzamukalay@uliege.be (J.B. Mukalay).

https://doi.org/10.1016/j.geodrs.2026.e01066
Received 6 October 2025; Received in revised form 12 January 2026; Accepted 25 February 2026
Available online 26 February 2026

et al., 2021; Koulibaly et al., 2015; Leão et al., 2020; Maroneze et al., 2014; Ramaroson et al., 2018; Saïdou et al., 2003), alongside the frequent presence of plinthite at or near the surface, as well as giant termite mounds (Adhikary et al., 2016; Alexandre, 2002; De Dapper and Malaisse, 1979; Malaisse, 2011; Mujinya et al., 2010).

The occurrence of plinthite on or close to the surface creates shallow or uncultivable soils with limited rooting volume, rendering these environments marginal or unsuitable for sustained agricultural production (Brogowski and Kwasowski, 2012; Coelho and Vidal-Torrado, 2000; Cooper et al., 2020; Dutta et al., 2003; Fauzi and Stoops, 2004; Fritsch et al., 2007; Jien et al., 2010; Kumar et al., 2019; le Roux et al., 2005; Legros, 2013; Loke et al., 2013; O'Brien et al., 2019; Ogunwole et al., 2001; Oluwatosin et al., 2020; Pereira-De-Oliveira et al., 2019). Plinthite is a clay material, rich in iron and poor in humus, which hardens irreversibly into ironstone through repeated wetting–drying cycles under solar radiation (WRB-IUSS, 2015). These soils exhibit several inherent limitations, including the development of compact layers, surface crusting, and restricted water percolation, all of which hinder their use for agricultural production (Bilong, 1992; De Azevedo and Bueno, 2017; Martins et al., 2018; Silva Martins et al., 2012; Wildemeersch et al., 2015; Yaro et al., 2008).

Population growth and the resulting increase in food demand have encouraged the cultivation of plinthite-affected soils (Oluwatosin et al., 2020). To mitigate the limitations, management strategies must be considered (Asiamah and Dwomo, 2010). Such strategies should aim to enhance soil water retention, reduce erosion, stimulate microbial activity, and improve thermal and gaseous exchanges, thereby supporting adequate air, water, and nutrient availability for crops.

In the Lubumbashi plain, however, the shallow presence of plinthite combined with the abundance of giant termite mounds, represents a major constraint to expanding cultivated areas. There are approximately 7 giant termite mounds per hectare, with an average spacing of 44.6 m and an average volume of 256 m^3 (Erens et al., 2015; Mujinya et al., 2014).

Their abundance and the high chemical quality of their materials (Baumgartner et al., 2021; de Lima et al., 2018; Enagbonma and Babalola, 2019; Eze et al., 2019; Jouquet et al., 2015; Kaschuk et al., 2006; Mujinya et al., 2013; Padonou et al., 2020; Rajeev and Sanjeev, 2011; Seymour et al., 2014) offer a valuable yet underutilized resource, particularly when these materials are spread onto soils previously loosened by subsoiling to break up and remove plinthite. This approach simultaneously increases soil thickness and enhances chemical fertility. Given this context, it is essential to assess how mechanical subsoiling and termite mound amendments may improve the properties of plinthite-affected soils.

This study is based on the hypothesis that: (1) incorporating termite mound materials increases soil depth and enhances soil fertility, thereby improving maize production, and (2) mechanical subsoiling improves soil water dynamics despite the presence of plinthite. The overall objective of this study is to evaluate the combined impact of subsoiling and termite mound materials on the fertility of Plinthosols cultivated with maize in the Lubumbashi region. More specifically, the study aims to: (i) characterize and map soil physicochemical properties to assess their spatial variability across the site; (ii) evaluate the influence of mechanical subsoiling on soil water dynamics; (iii) assess the combined effects of subsoiling and termite mound amendments on maize grain yield; and (iv) use regression models to identify the key soil variables explaining yield variability.

2. Methodology

2.1. Site description

This study was conducted at FarmCo, located on the outskirts of Lubumbashi, approximately 60 km east of the city along the Kasenga road in the Kifumanshi River valley. The study area is situated between 27.756781° and 27.790340° E and 11.411949° and 11.441744° S, at an elevation ranging from 1150 to 1200 m a.s.l. (Fig. 1). It covers 660 **ha** of land dominated by Plinthosols according to the WRB classification (WRB-IUSS, 2015).

At this site, systematic excavation of the lateritic surface layers, combined with mechanical subsoiling to fragment and remove plinthite, was carried out across the entire study area during the 2021–2022 cropping season, prior to soil sampling and yield measurements. Before subsoiling, the plinthic crust occurred at depths of less than 10 cm over nearly one quarter of the site, severely limiting the effective rooting depth. The subsoiling operation was performed using a three-tine subsoiler at a minimum working depth of 40 cm to break compact plinthic layers and increase the effective rooting depth. In parallel, materials from inactive *Macrotermes falciger* termite mounds—abundant throughout the area—were completely removed and spread over the loosened plots to expand arable land, facilitate machinery operations, and serve as a soil amendment (Fig. 2). FarmCo is one of the largest farms in the Lubumbashi region and is renowned for its large-scale production of maize grain for human consumption.

The outskirts of Lubumbashi have a C_{W6} climate according to the Köppen classification, characterized by a dry season (May–September), a rainy season (November–March), and two transition months (April and October) (Assani, 1999). The mean annual rainfall is 1270 mm and the mean annual temperature is 20.1 °**C**, with minimum temperatures around 8 °**C** during the coldest month and maximum temperatures reaching 32 °**C** during the hottest month (Malaisse, 2011).

2.2. Sampling and laboratory analysis

Transect sampling was carried out across the entire study area, covering 660 **ha** and subdivided into 10 blocks (B1-10). Disturbed soil samples were collected using a soil auger in the 0-10 cm layer, at 200 m intervals following a zigzag sampling design during the WRB, 2022–2023 growing season, after the implementation of subsoiling and the incorporation of termite mound materials. In areas where the soil was shallow (<40 cm), the effective soil depth was measured with the auger down to the plinthite layer. A total of 207 disturbed samples were collected (Fig. 3), air-dried for five days, sieved to 2 mm, and prepared according to ISO 11074 standards for chemical analysis.

Soil analyses were performed at the soil chemistry laboratory of Gembloux Agro-Bio Tech, (Belgium). The analyses included: measurement of pH in water and in 1 N KCl; determination of total organic carbon (TOC) using the Walkley–Black wet oxidation method (Walkley and Black, 1934); and quantification of available elements after extraction with ammonium acetate + EDTA (ethylene diamine tetra acetic acid) at pH 4.65. The resulting extracts were analysed using a colourimeter for phosphorus concentration and ICP-OES (inductively coupled plasma–optical emission spectrometry) for calcium, magnesium, and potassium, and trace elements (copper, iron, aluminium, and manganese).

In addition, a detailed description of representative ±1 m-deep soil profiles was carried out in accordance with the soil description guidelines of the World Reference Base for Soil Resources (WRB, 2022). Soil samples were taken from the diagnostic horizons for physicochemical analysis. Undisturbed samples were collected from these horizons using Kopecky cylinders. These samples were then sent to the laboratory for bulk density measurement and soil water hydraulic analysis at the Soil Physics and Mechanics Technical Platform (PhyMeSol), Agro-Bio Tech, Belgium. Saturated hydraulic conductivity (Ksat) was measured using a constant head permeameter, and soil water retention was determined using the Richard apparatus.

2.3. Cross-validation

Geostatistical analyses were performed to present the results in spatial form using maps. To this end, several interpolation methods

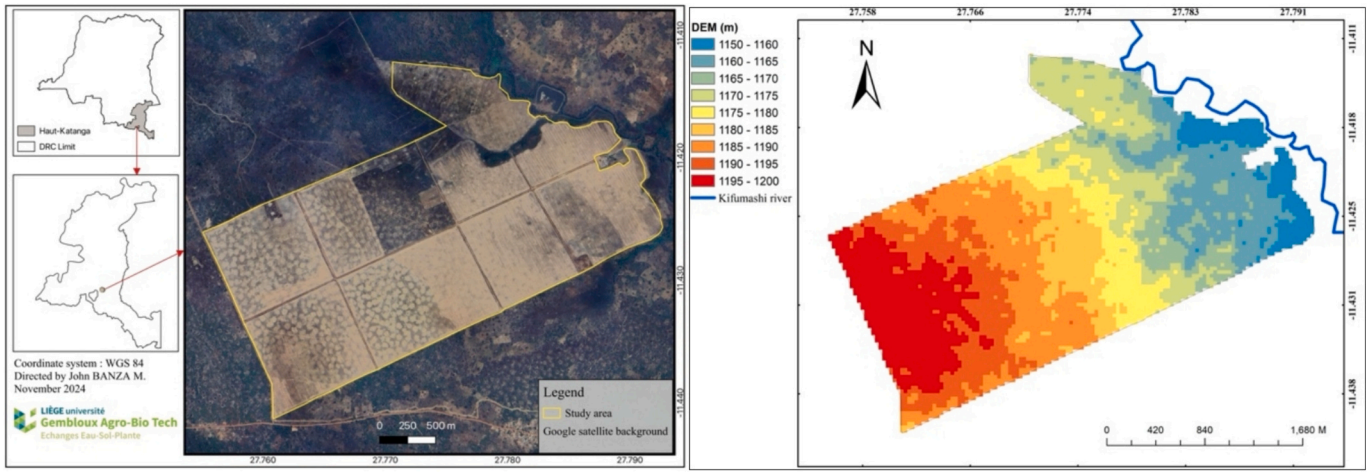

Fig. 1. Left: Location of the study site (FarmCo) in Lubumbashi area, Haut-Katanga Province, Democratic Republic of Congo. Right: STRM-DEM (30 m resolution) showing the topographic variability across the study area.

Fig. 2. A: Drone image showing levelled termite mounds (white patches), B: collection and transport of plinthite fragments after subsoiling, and C: plinthite stored outside the cultivated plots (photo credit: John Banza M.).

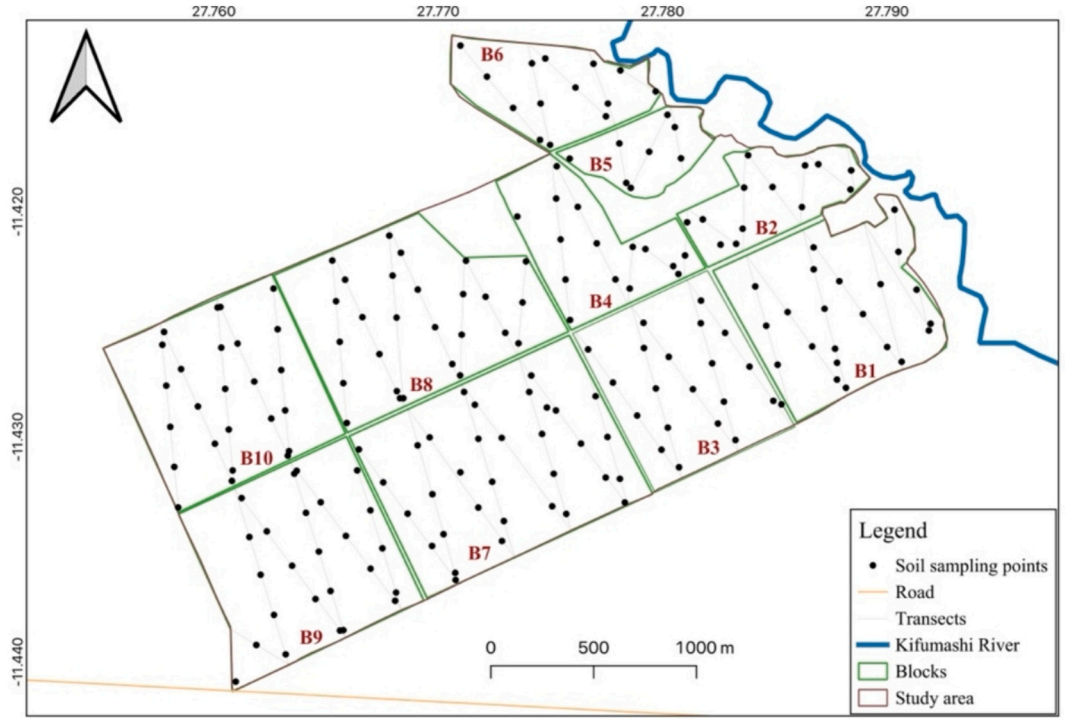

Fig. 3. Soil sampling plan for the study area.

available in ArcGIS 10.8.1 were evaluated (Johnston et al., **2001**). After processing, the semivariogram generated for kriging did not show clear or stable spatial dependence in the dataset (Fig. S.1-S.3). The Inverse Distance Weighted and Spline models showed poor agreement between observed and predicted values, sometimes producing a pronounced "bull's-eye" artefact. Only the Natural Neighbor and Spline With Barriers models produced spatially realistic and coherent patterns. To differentiate between these two methods, cross-validation was performed using ModelBuilder. This validation included 100 Monte Carlo repetitions for each model, using 90% of the randomly selected data for calibration and 10% for validation. This procedure was applied to each spatially represented variable. The performance of each interpolation method was evaluated using the root mean square error (RMSE, Eq. 1) (Smith and Smith, **2007**) and the bias (Eq. 2) (Harwell, **2018**). RMSE indicates the dispersion or variability of prediction errors, while bias assesses systematic over- or underestimation by the model. These measures were determined as follows:

$$RMSE = \sqrt{\frac{1}{n}\sum_{i=1}^{n}\left(P_{obs\ (i)} - P_{pred(i)}\right)^2} \quad (1)$$

$$Bias = \frac{1}{n}\sum_{i=1}^{n}\left(P_{obs\ (i)} - P_{pred(i)}\right) \quad (2)$$

Where: RMSE is the root mean square error, n is the total number of validation samples; $P_{obs(i)}$ is the value of the i-th observation, and $P_{pred(i)}$ is the corresponding predicted value. Bias: the bias is better when it is close to zero.

After cross-validation, the Spline With Barriers model outperformed all other tested interpolators, exhibiting low median RMSE values and low, often zero, bias (Fig. S.4). Consequently, this interpolation method was applied to the full dataset (100%) for all the mapped variables.

2.4. Determination of yield

The grain yield of maize was measured in 1 m^2 quadrats, with at least five replicates per block, following the formula of Tandzi and Mutengwa (**2020**) (Eq. 3). This method is considered one of the simplest and most rapid for on-farm yield estimation (Sapkota et al., **2016**). A total of 41 yield plots were established (Fig. 4), and the same sampling locations were used for both growing seasons (2022–2023 and 2023–2024) to ensure temporal comparability of yield measurements. Yield was standardized to a grain moisture content of 13%. Regarding crop management at the site, aside from subsoiling and the application of termite mound material, operations included mechanized soil preparation (plowing and harrowing), sowing, mineral fertilization, and pre-emergence herbicide application, all applied uniformly across all blocks. Maize sowing was carried out simultaneously with the application of an NPK (10—20—10) base fertilizer at a rate of 200 kg ha^{-1}, followed by urea topdressing applied 45 days after sowing, also 200 kg ha^{-1}. A single maize variety was cultivated at spacings of 0.75 m between rows and 0.25 m within rows, corresponding to a planting density of 53,333 plants ha^{-1}.

$$\text{Yield (kg/ha)} = \left[\left(\text{number of rows of grain per earX } \frac{\text{number of ears per m}^2}{100}\right) X \left(\text{Weight of 1000} - \frac{\text{grains (g)}}{10000}\right) X\ 10000\right] \quad (3)$$

2.5. Stepwise linear regression

Stepwise multiple linear regression analyses were conducted to

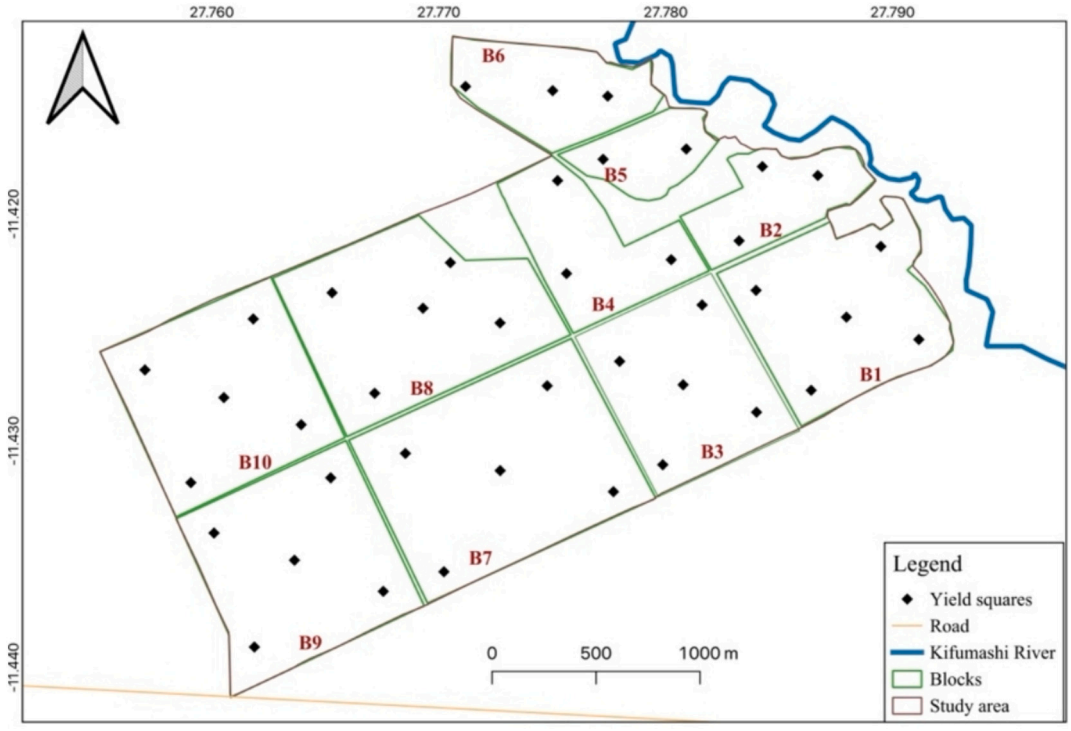

Fig. 4. Spatial distribution of maize grain yield sampling plots across the study area. Sampling plots are shown within each block (B1–B10).

identify the soil factors influencing maize grain yield. Prior to regression modelling, Spearman's rank correlations and principal component analysis (PCA) were performed to explore the relationships between soil variables and yield. These preliminary analyses helped restrict the set of explanatory variables to those showing significant associations with yield, and these variables were subsequently used in the regression models.

Variable selection was performed using both forward and backward stepwise procedures. The optimal model was chosen based on Akaike's information criteria (AIC), with the model presenting the lowest AIC retained as it provides the best balance between goodness of fit and model parsimony (Venables and Ripley, 2002). The variance inflation factor (VIF) was the then computed to assess multicollinearity among predictors (Akinwande et al., 2015), and only variables with VIF <3 were included in the final model (O'Brien et al., 2019). In addition, model performance was evaluated using RMSE and *p*-values, with statistical significance set at $p < 0.05$ (Smith and Smith, 2007). The polynomial regression equation was computed to obtain unstandardized coefficients, which represent the direct effect of each explanatory variable on yield in their original measurement units. The equations were also used to compare predicted versus observed maize grain yields, based on pixel values from the maize grain yield map and field-measured yields. Furthermore, standardized beta coefficients and their 95% confidence intervals were calculated to assess the strength and direction of the relationship between each predictor and yield (Nieminen, 2022). All statistical analyses were performed using R Studio software (version 4.4.1) and the R statistical environment (R Core Team, 2025).

Fig. 5 illustrates the methodological workflow used for soil characterization and crop yield analysis at the study site. The procedure integrates field sampling, laboratory analyses, data structuring and geostatistical modelling. Soil properties (0–10 cm and profile horizons) were analysed using both disturbed and undisturbed samples, followed by spatial interpolation and model cross-validation. These outputs were subsequently linked to maize yield data to generate soil property and yield maps.

3. Results

3.1. Assessment of the effectiveness of subsoiling on soil depth

Consistent with the initial site conditions, where the plinthic crust occurred at very shallow depths across much of the study area, several zones still exhibited very shallow soil layers after subsoiling. Fig. 6 illustrates the spatial distribution of soil thickness after mechanical subsoiling across the entire study area. The map highlights zones with very shallow soil layers, in some cases less than 9 cm thick, where the subsoil locally outcrops at the surface, indicating the need for additional subsoiling operations in these areas. The thinnest soils are mainly concentrated in the central part of the concession, reflecting the strong spatial heterogeneity of soil depth despite the applied subsoiling treatment. In contrast, only blocks B2, B5, B6, and B9 are entirely characterized by deep soils, with soil thickness exceeding 73 cm.

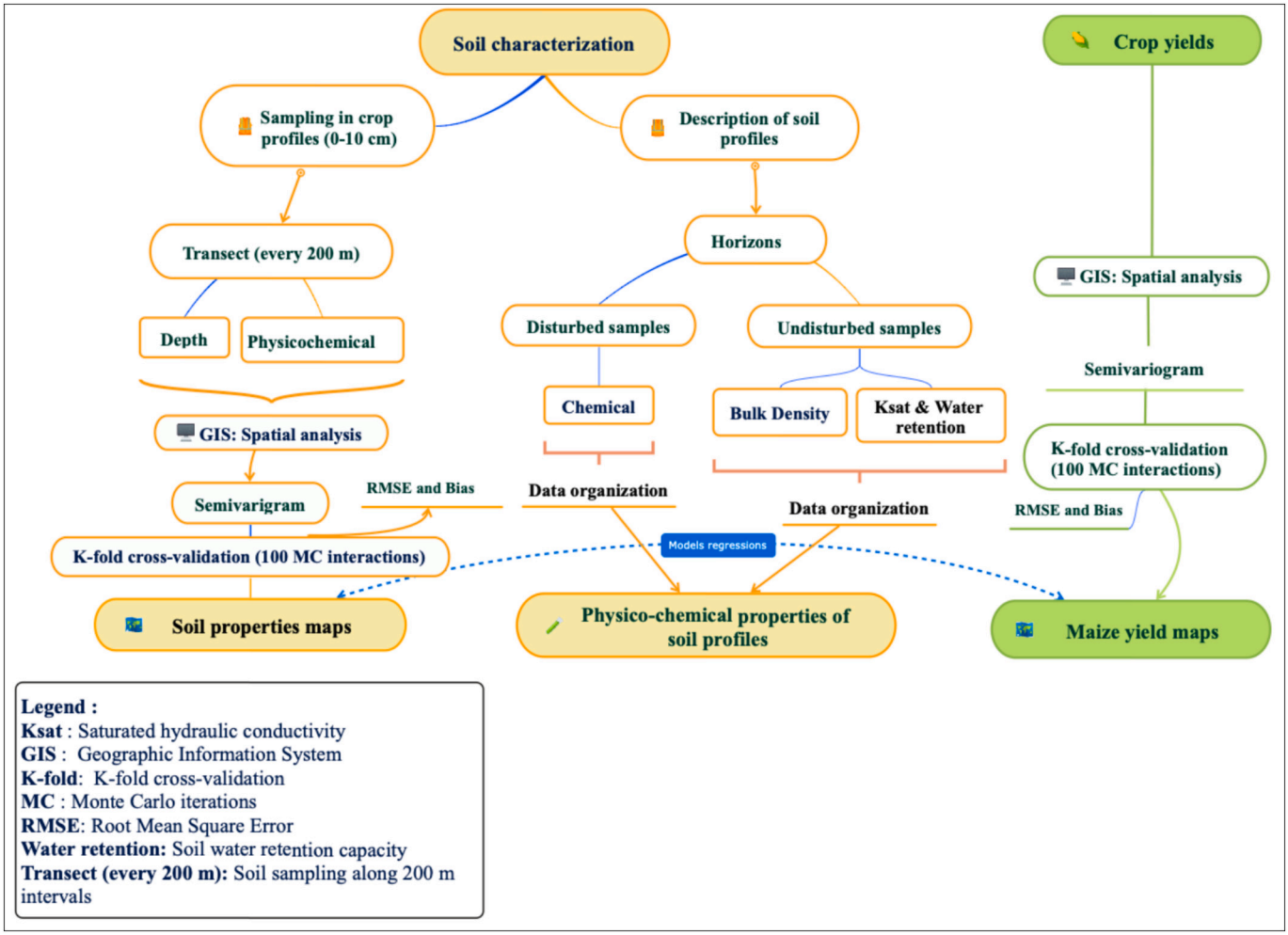

Fig. 5. Methodological workflow for soil characterization and crop yield analysis.

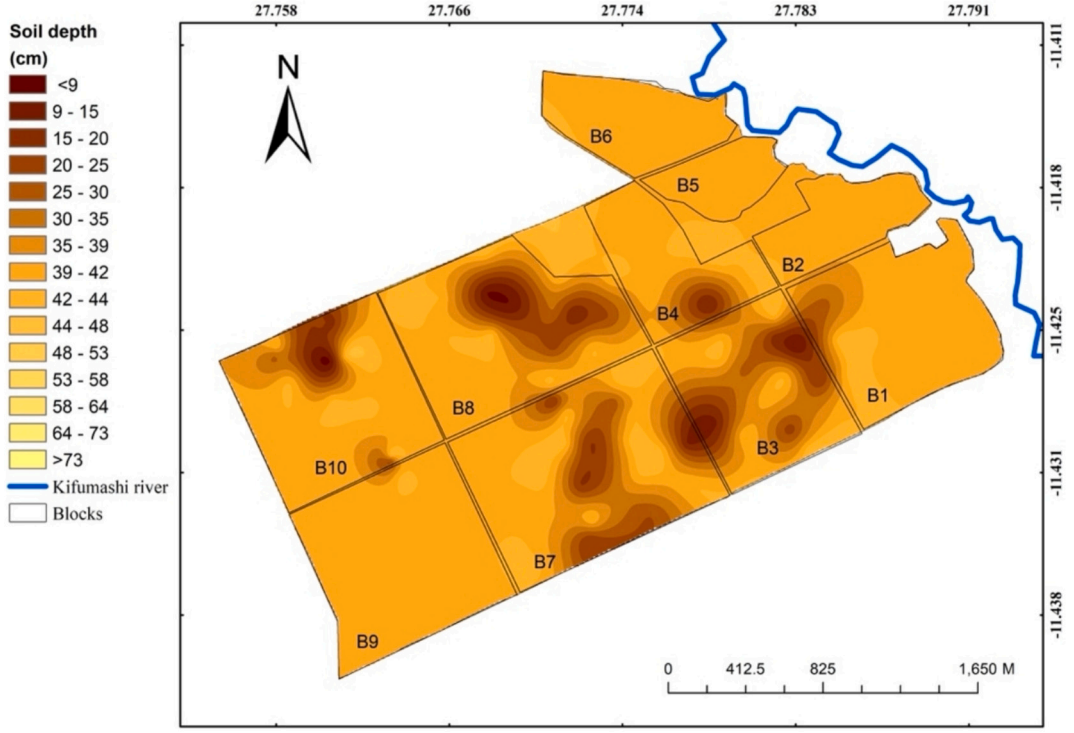

Fig. 6. Spatial variation in soil thickness across the study area after subsoiling. B denotes the different blocks (B1-B10).

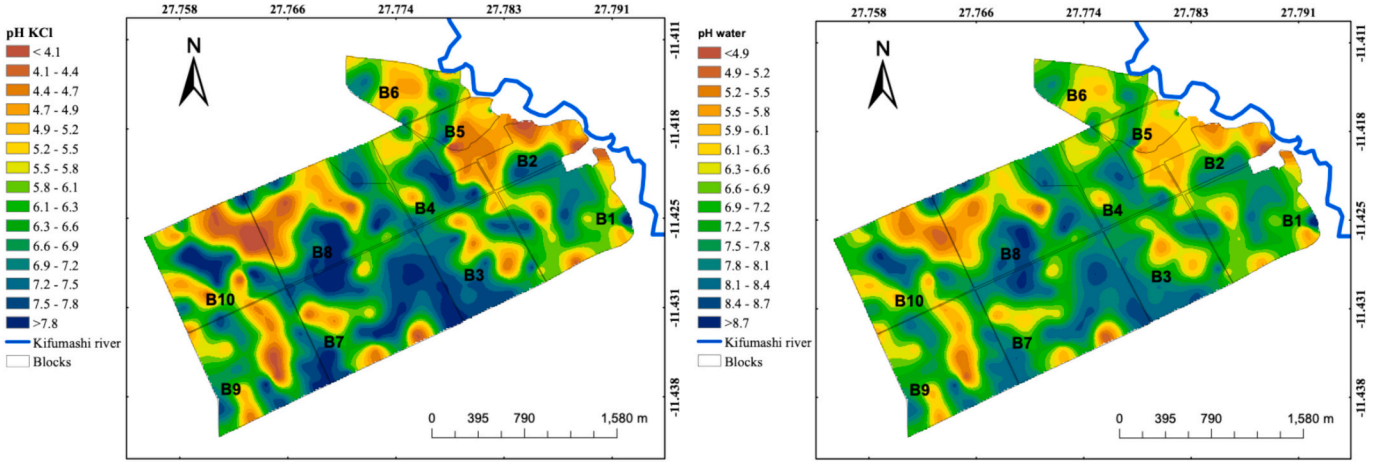

Fig. 7. Spatial variation of soil pH measured in KCl (left) and in water (right) in the 0–10 cm layer after subsoiling and application of termite mound material. B denotes the blocks (B1–B10).

3.2. Spatial variation in soil chemical properties after subsoiling and spreading of termite mound material

3.2.1. Soil pH

Fig. 7 shows the spatial distribution of soil pH measured in KCl (left) and in water (right) in the surface layers (0-10 cm) after mechanical subsoiling and the application of termite mound material. The pH KCl map highlights areas with values lower than 4.1 and higher than 7.8, distributed across the study area. Its spatial pattern is highly heterogeneous, with more pronounced soil acidification observed in blocks B8, B9, and B10, as well as in the northern part of the site near the river. In contrast, the central part of the site generally exhibits pH KCl values above 5.5, indicating less acidic to near-neutral soil conditions. A similar spatial pattern is observed for pH measured in water, although localized extremes with values below 4.9 and above 8.7 occur in specific areas within the study perimeter.

3.2.2. Total organic carbon

Fig. 8 shows the spatial variation of total organic carbon (TOC) in the surface layer (0–10 cm) after mechanical subsoiling and application of termite mound material. TOC values range from less than 0.4% to more than 2.5%, depending on location. Overall, the study area is characterized by generally low TOC contents, with only a few localized zones exceeding 2.5%, mainly within specific blocks. A slight increase in TOC is observed near the river, suggesting more favourable conditions for organic matter accumulation in this zone; however, these values remain moderate relative to the rest of the study area.

3.2.3. Available nutrients

The results presented in Fig. 9 illustrate the spatial distribution of

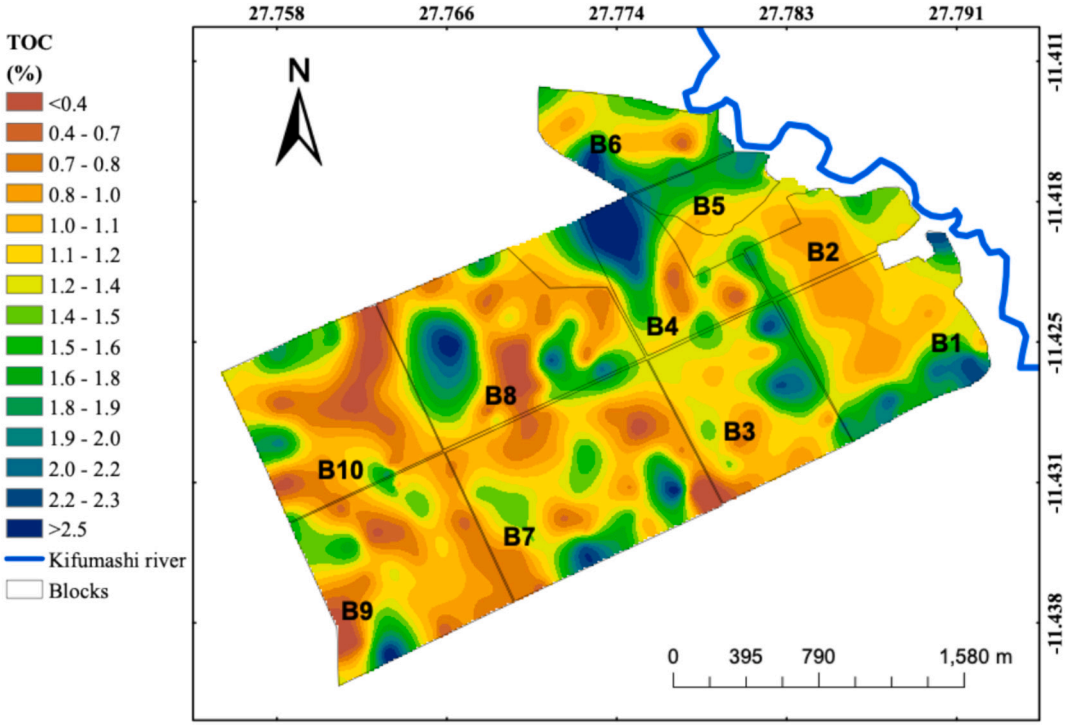

Fig. 8. Spatial distribution of total organic carbon (TOC) in the 0–10 cm soil layer after subsoiling and application of termite mound material. B denotes the blocks (B1–B10).

available nutrients in the surface layer (0–10 cm) after mechanical subsoiling and amendment with termite mound material. Available phosphorus contents range from less than 5.1 mg kg^{-1} to more than 145.5 mg kg^{-1} across the study area. The highest concentrations are observed in blocks B10, B7, and B4, whereas a general decrease in P availability occurs toward the peripheral zones of the study site, with a few localized exceptions (Fig. 9a).

Calcium concentrations vary from less than 1361 to more than 18,268 mg kg^{-1}, showing a generally homogeneous spatial distribution, although localized enrichment is observed in blocks B8, B9, and B10 (Fig. 9b). Available aluminium ranges from less than 44.4 mg kg^{-1} to more than 293.4 mg kg^{-1}, with higher contents in blocks B8, B9, and B10, as well as near the river in blocks B1 and B2 (Fig. 9c).

Copper concentrations range from less than 1.9 mg kg^{-1} to more than 25.8 mg kg^{-1}, displaying a relatively uniform distribution over the study area. Only localized enrichment is observed at the downstream end of block B1 near the river, where values reach 25.8 mg kg^{-1} (Fig. 9d). Potassium concentrations range from less than 130.2 mg kg^{-1} to more than 942.0 mg kg^{-1}, with a general decreasing trend toward lower-altitude areas close to the river, although elevated values persist at the northeastern extremity of block B1 (Fig. 9e).

Iron contents range from less than 28.1 mg kg^{-1} to more than 351.7 mg kg^{-1}, with an overall irregular spatial distribution. The dominant class lies between 77.8 and 102.7 mg kg^{-1}, while maximum concentrations occur locally in small zones within blocks B3 and B10 (Fig. 9f). Magnesium varies from less than 238.8 mg kg^{-1} to more than 2987 mg kg^{-1} and shows a markedly heterogeneous spatial pattern, with higher concentrations mainly in blocks B4 and B10 (Fig. 9g). Finally, manganese ranges from less than 4.4 mg kg^{-1} to more than 669.4 mg kg^{-1}, with an irregular distribution and a tendency to increase with distance from the river, particularly in blocks B10, B9, B8, B7, B3, and B1 (Fig. 9h).

3.3. Physicochemical characterization of soil profiles

Data on the physicochemical properties of soils after mechanical subsoiling and amendment with termite mound material reveal pronounced heterogeneity among soil profiles and horizon depths. Soil pH measured in water ranges from 5.7 to 8.4, indicating slightly acidic to slightly alkaline conditions, which are generally favourable for nutrient availability and plant uptake. In contrast, pH measured in KCl varies between 4.2 and 7.6, reflecting the presence of exchangeable acidity within the soil exchange complex.

Total organic carbon (TOC) contents show substantial vertical and lateral variability, reaching values of up to 2.9% in the surface horizon (Ap) of profile B7, indicating locally enhanced organic matter levels in the topsoil. Available phosphorus contents are generally low, ranging from 0.3 to 154.8 mg kg^{-1}, with maximum values observed in profile B10, suggesting enhanced P availability within the effective rooting zone.

Calcium concentrations are particularly high, especially in the Ap horizon of profile B4 (12,499 mg kg^{-1}), while remaining moderately to highly abundant in the other profiles. Potassium and magnesium contents reached maximum values of 486.6 mg kg^{-1} and 795.2 mg kg^{-1} in surface soils, respectively, illustrating the positive contribution of termite mound amendments to the supply of base cations.

Manganese exhibits a contrasting vertical distribution, with maximum concentrations of 190 mg kg^{-1} at depth in profile B5, whereas in most other profiles the highest Mn values occur in the surface horizons (Ap). Copper and iron display similar depth-dependent trends, with concentrations decreasing downward in the soil profile, suggesting a strong control of surface processes on micronutrient dynamics. In contrast, aluminium shows relatively higher concentrations in deeper horizons, consistent with the influence of plinthitic materials.

Analysis of horizon stratification (Ap, AB, Bs) reveals an overall decline in nutrient contents with increasing depth, reflecting the persistent influence of plinthite on soil functioning, which reduces the effective rooting volume and may limit the long-term sustainability of agricultural productivity. Particle-size distribution analysis indicates textures dominated sandy loam to clay loam textures, with a marked vertical gradient characterized by increasing clay contents in subsurface horizons (e.g., profile B5: from 18.6% in Ap to 37.6% and 44% in deeper

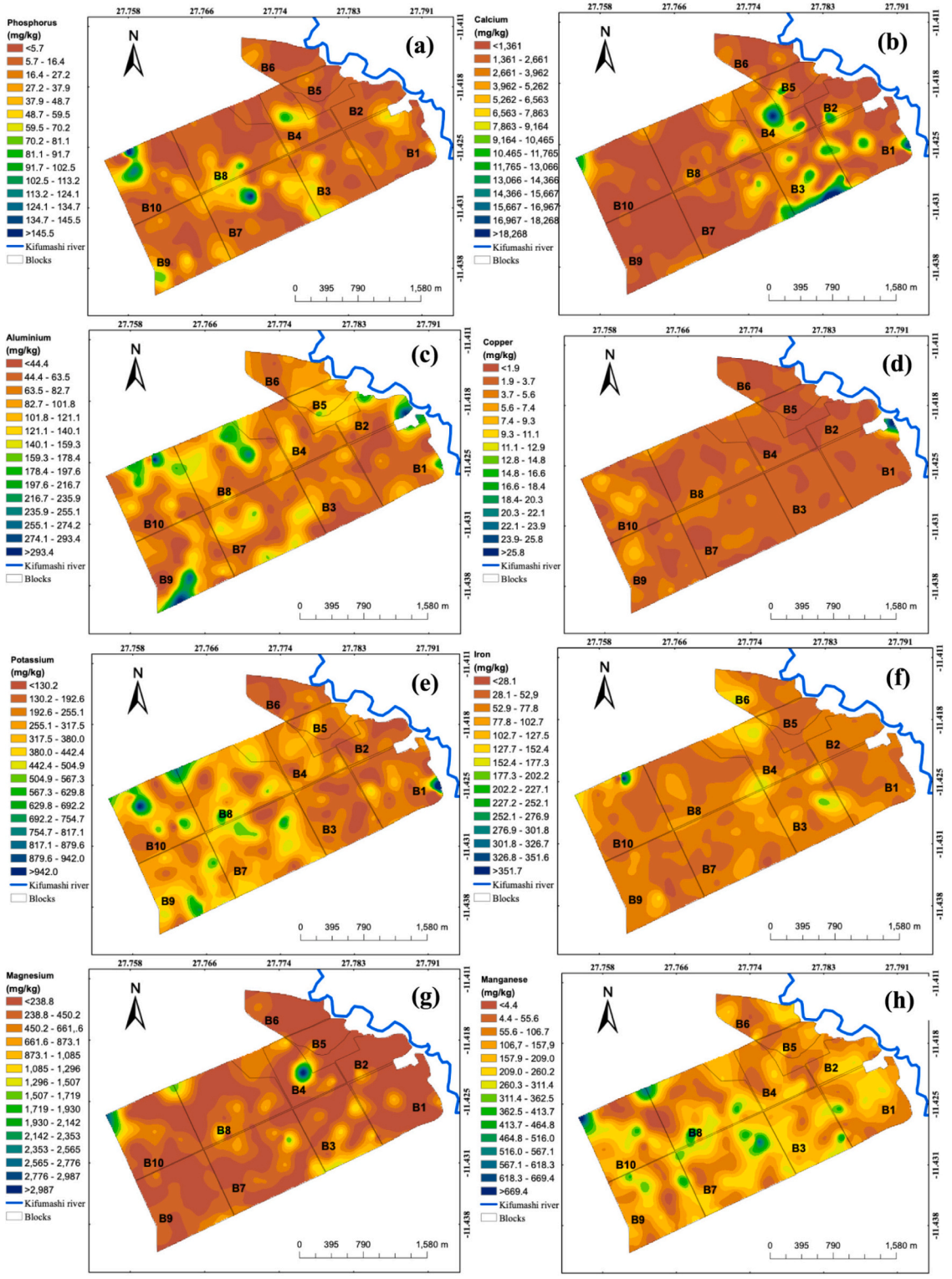

Fig. 9. Spatial variation of available soil nutrients in the 0–10 cm layer after subsoiling and application of termite mound material: (a) P, (b) Ca, (c) Al, (d) Cu, (e) K, (f) Fe, (g) Mg, and (h) Mn. B denotes the blocks (B1–B10).

horizons; profile B6: from 19.7% to 40.2% and then 34.6%). This pattern is typical of clay illuviation processes associated with plinthitic soils.

Surface horizons (Ap) show higher sand contents in certain blocks (B1, B6, B8, and B10, with 40–47% sand), whereas other surface horizons (B4, B5, B7, and B9) are dominated by silt (≥50%). In deeper horizons (AB, Bs, and Bcs), clay proportions generally increase, resulting in denser soil layers and reflecting the structural and textural control exerted by plinthite on soil profile differentiation (Table 1).

3.4. Influence of subsoiling on bulk density and water dynamics in soil profiles

The results show that bulk density (BD) is generally lower in surface horizons, ranging from 1.17 to 1.53 g cm^{-3}, and increases with depth

Table 1
Physicochemical properties of soil profiles after mechanical subsoiling and amendment with termite mound materials.

Profiles	Horizons	Depth	pH water	pH KCl	TOC	P	Ca	K	Mg	Mn	Cu	Fe	Al	Clay	Silt	Sand
		(cm)			(%)	(mg kg^{-1})									(%)	
B1	Ap	0-26	8.2	7.5	0.9	1.3	2546	205.3	201.5	189.9	2.6	51.4	48.3	19.4	33.2	47.4
B2	Ap	0-27	6.9	5.6	0.8	0.4	875.3	62.7	77.8	117.5	1.8	44.8	49.9	21.1	40.4	38.5
	AB	27-79	5.6	4.2	0.2	0.3	266.2	71.5	50.4	30.5	0.5	14.6	147.4	28.4	37.7	33.9
B3	Ap	0-30	7.9	7.6	1.1	8.9	2566	96.1	358.1	194.8	3.4	55.7	66.9	22.2	47.6	30.2
	AB	30-43	6.0	4.9	0.6	2.4	245.2	63.6	126.0	27.4	1.0	20.5	97.6	20.0	45.2	34.8
	Bs	43-80	5.5	4.3	0.4	1.9	82.7	134.9	148.3	26.5	0.7	18.3	133.4	30.6	44.5	24.9
B4	Ap	0-20	8.4	7.3	1.2	13.9	12,499	218.9	795.2	166.9	3.9	72.7	52.0	24.1	57.9	18.0
	AB	20-35	8.0	7.6	1.8	19.0	2651	70.6	260.4	39.8	2.6	43.6	67.4	16.1	52.3	31.6
B5	Ap	0-46	6.1	5.2	2.0	1.1	1735	244.8	375.9	16.4	2.1	67.8	94.3	18.6	56.0	25.4
	AB	46-92	7.2	5.4	0.4	1.0	1101	113.5	109.9	31.0	0.6	8.1	65.7	37.6	30.2	32.2
	Bs	92-150	7.8	6.4	0.2	4.3	1331	148.4	386.0	190.0	0.3	22.5	87.7	44.0	27.2	28.8
B6	Ap	0-25	5.9	4.8	1.2	2.0	514.2	144.9	86.9	104.5	1.0	30.4	113.9	19.7	32.9	47.4
	AB	25-132	6.1	4.8	0.2	0.6	442.8	238.1	143.9	102.5	0.4	22.3	115.0	40.2	28.1	31.7
	Bs	132-201	5.7	4.2	0.2	2.7	190.5	147.2	209.3	20.1	0.3	7.8	134.5	34.6	38.0	27.4
B7	Ap	0-20	8.0	7.6	2.9	44.7	4856	324.2	459.1	197.9	3.3	123.4	132.6	20.6	50.5	28.9
	AB	20-30	6.5	5.9	0.9	3.8	298.0	188.2	169.4	91.9	1.5	26.9	78.8	18.0	51.7	30.3
	Bs	30-75	5.6	4.4	0.4	1.5	97.8	160.3	101.4	75.1	0.6	23.6	112.0	24.3	51.3	24.4
	Bsx	>75	5.6	5.2	0.3	1.7	152.3	115.3	157.7	49.6	0.5	17.1	105.5	–	–	–
B8	Ap	0-35	6.0	4.8	0.7	3.4	165.6	101.5	122.2	34.5	1.9	24.7	94.1	18.8	41.2	40.0
	Bcs	35-110	6.1	4.2	0.2	1.5	27.0	119.5	69.5	10.4	0.9	10.2	233.6	34.1	45.0	20.9
B9	Ap	0-30	7.1	6.4	1.4	8.7	746.3	121.8	240.4	128.1	3.4	76.4	82.7	22.2	53.2	24.6
	Bcs1	30-70	5.3	4.2	0.7	2.9	90.3	125.2	110.8	58.2	1.9	34.4	194.6	27.8	49.6	22.6
	Bcs2	>70	5.5	4.5	0.3	1.1	71.3	310.2	177.4	27.4	1.1	23.6	135.9	–	–	–
B10	Ap	0-27	7.5	6.7	2.3	154.8	1818	486.6	446.4	47.8	2.1	97.2	168.2	12.0	43.5	44.5
	Bs	27-130	7.0	5.4	0.3	3.7	75.8	524.5	80.9	3.1	0.3	17.2	80.9	21.8	46.4	31.8

Soil pH was measured in water and 1 N KCl; total organic carbon (TOC) was determined using the Walkley–Black method (Walkley and Black, **1934**); available elements were extracted with ammonium acetate + EDTA (pH 4.65) and analysed by ICP-OES; phosphorus was determined colourimetrically; particle-size distribution was determined using the pipette method.

Table 2
Bulk density (BD), saturated hydraulic conductivity (Ksat), field capacity water content (DUL), and wilting point water content (LL) in soil profiles across the study site.

Profile	Horizon	Depth	BD	Ksat	DUL	LL
		(cm)	(g cm^{-3})	(mm day^{-1})	(v/v)	
Block 1	Ap	0-26	1.35	7780	0.26	0.16
Block 2	Ap	0-27	1.53	51.7	0.22	0.16
	AB	27-79	1.5	664	0.24	0.20
Block 3	Ap	0-30	1.56	86.4	0.19	0.11
	AB	30-43	1.85	6130	0.15	0.08
	Bs	43-80	1.92	7780	0.14	0.09
Block 4	AP	0-20	1.46	125	0.23	0.18
	AB	20-35	1.19	126	0.26	0.19
Block 5	Ap	0-46	1.19	625	0.30	0.24
	AB	46-92	1.7	276	0.24	0.20
	BS	92-150	1.77	63.9	0.27	0.23
Block 6	Ap	0-25	1.37	333	0.21	0.14
	AB	25-132	1.65	32.9	0.19	0.15
	Bs	132-201	–	–	–	–
Block 7	Ap	0-20	1.42	1210	0.26	0.16
	AB	20-30	1.66	4320	0.18	0.09
	Bs	30-75	1.92	864	0.15	0.09
	Bsx	>75	–	–	–	–
Block 8	Ap	0-35	1.46	44.7	0.16	0.10
	Bcs	35-110	1.74	400.5	0.12	0.06
Block 9	Ap	0-30	1.17	1810	0.26	0.09
	Bcs1	30-70	1.46	892.4	0.19	0.09
	Bcs2	>70	–	–	–	–
Block 10	Ap	0-27	1.45	1410	0.18	0.13
	BS	27-130	1.62	767	0.21	0.16

toward more compact plinthic horizons, where values exceed 1.70 g cm^{-3}. This vertical pattern reflects a structural improvement of surface soils, likely associated with mechanical subsoiling and amendment with termite mound material.

Saturated hydraulic conductivity (Ksat) exhibits strong vertical and lateral variability, with very high values in surface horizons (ranging from 1810 to 7780 mm day^{-1} in profiles B1, B3, and B9) and substantially lower values at depth, particularly in plinthic horizons (e.g., 63.9 mm day^{-1} in the Bs horizon of profile B5).

Soil water retention at field capacity (drained upper limit, DUL) is higher in surface horizons (ranging from 0.257 to 0.302 *v*/v) and declines markedly in plinthic horizons (from 0.115 to 0.154 v/v). In contrast, the wilting point (lower limit, LL) remains relatively high, reaching values of up to 0.226 v/v, thereby reducing the amount of plant-available water within the soil profile (Table 2).

3.5. Spatial variation in grain maize yield after subsoiling and spreading termite mound material

Fig. 10 shows the spatial distribution of grain maize yield across the study area after mechanical subsoiling and amendment with termite mound material for the 2022–2023 (left) and 2023–2024 (right) growing seasons. Grain yield values range from less than 2.3 to more than 11.1 t ha^{-1}, depending on location within the study perimeter. During the first growing season (2022–2023), yield patterns are spatially heterogeneous, with lower yields predominantly observed in blocks B8 and B10, whereas the remaining blocks generally exhibit moderate to high yields, particularly in low-lying areas close to the river.

During the second growing season (2023–2024), a general increase in maize grain yield was observed across all blocks, with an average improvement of approximately 1 t ha^{-1}. Although blocks B8 and B10 largely maintained their lower-yield patterns, several localized zones within these blocks showed marked yield improvement. This overall increase resulted in a rise in the mean grain yield from 7.1 to 8.2 t ha^{-1}, highlighting the positive cumulative effect of subsoiling and termite mound amendments over time (Fig. 11).

3.6. Interactions between soil parameters and maize yield

Correlation analyses conducted across both growing seasons revealed that higher soil pH values, together with greater concentrations of total organic carbon (TOC) and calcium (Ca), were generally

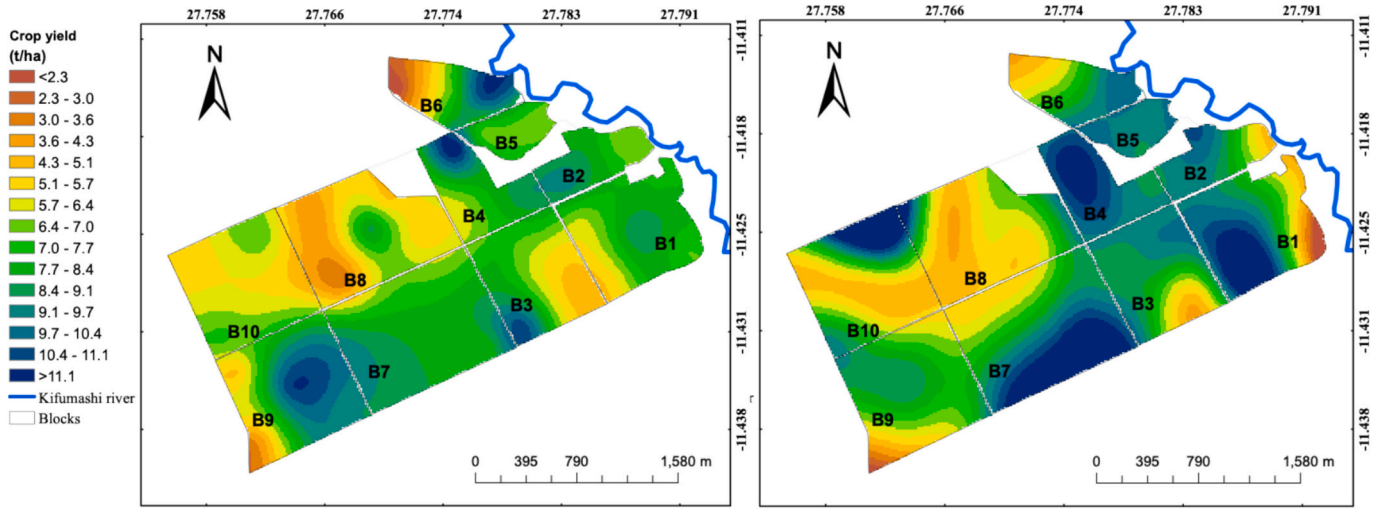

Fig. 10. Spatial distribution of grain maize yield across the study area after subsoiling and amendment with termite mound material. Left: 2022–2023 growing season; right: 2023–2024 growing season. B denotes the blocks (B1–B10).

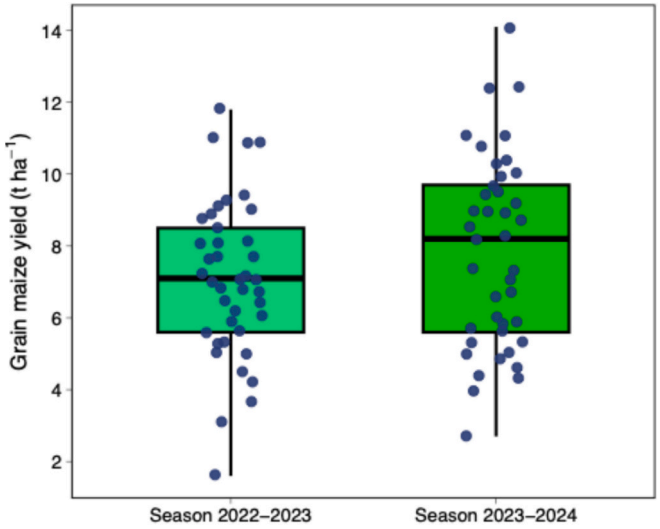

Fig. 11. Descriptive analysis of grain maize yield across the study area for the 2022–2023 and 2023–2024 growing seasons. Boxes represent the interquartile range, horizontal lines indicate median values, and points correspond to individual yield observations.

associated with increased maize grain yields. In contrast, copper (Cu) concentrations showed a consistent negative correlation with yield, an effect that was particularly pronounced during the first growing season (Fig. 12).

These relationships were further supported by principal component analysis (PCA). The first principal axis (PC1, explaining 27.6% of the total variance) represents a soil fertility gradient dominated by pH, Ca, and organic matter, along which maize yields (Rdt1 and Rdt2) were positively associated with pH measured in water and KCl, Ca, and TOC, and negatively associated with Cu.

The second principal axis (PC2, explaining 23.6% of the variance) contrasts a Mn–K–P–Mg–depth gradient with Fe and Al, and accounts for a smaller proportion of yield variability. Along this axis, Rdt2 exhibited a weak negative relationship with Mn, suggesting a secondary influence of certain micronutrients on yield performance.

Overall, the spatial variability of maize grain yield was primarily structured by the edaphic gradient represented by PC1. Together, the first two PCA axes explain 51.2% of the total variance, indicating that additional factors not captured by the measured soil variables also contribute to yield variability across the study area (Fig. 13).

3.7. *Performance of grain maize yield regression models derived from stepwise linear regression*

Grain maize yields in the study area, as explained by stepwise multiple linear regression models, indicate that several soil properties exert a significant influence on crop production. The models exhibit coefficients of determination (R^2) greater than 0.50, *p*-values <0.05, and RMSE values lower than 1, demonstrating a satisfactory capacity to explain yield variability. However, regression models derived from yield map pixel values (Fig. 14a) show slightly lower R^2 values than those based on field-measured yields (Fig. 14b), suggesting that models calibrated with field observations provide more robust predictions.

For yields estimated from pixel-based values, soil pH measured in KCl and Fe were identified as the main determinants during the first growing season. Standardized beta coefficients indicate that a one-standard-deviation increase in Fe concentration is associated with a 0.153 standard-deviation decrease in yield, whereas a one-standard-deviation increase in pH KCl corresponds to a 0.075 standard-deviation increase in yield (Fig. 14c). During the second growing season, copper (Cu) and calcium (Ca) emerged as the dominant explanatory variables (Fig. 14d).

Regression models based on field-measured yields further confirm the significant role of specific soil properties. During the first season, soil pH, manganese (Mn), copper (Cu), and calcium (Ca) were identified as key determinants. Both Cu and Mn show negative relationships with yield, while a one-standard-deviation increase in soil pH and Ca results in yield increases of 0.334 and 0.332 standard deviations, respectively (Fig. 14e). During the second season, soil pH, Mn, and total organic carbon (TOC) were retained in the optimal model. In this case, a one-standard-deviation increase in Mn is associated with a 0.35 standard-deviation decrease in yield, whereas equivalent increases in pH and TOC correspond to yield increases of 0.21 and 0.29 standard deviations, respectively (Fig. 14f).

4. Discussion

4.1. *Analysis of the performance of the interpolation model used*

In this study, the Spline With Barriers interpolation model outperformed all other tested methods, producing more realistic and

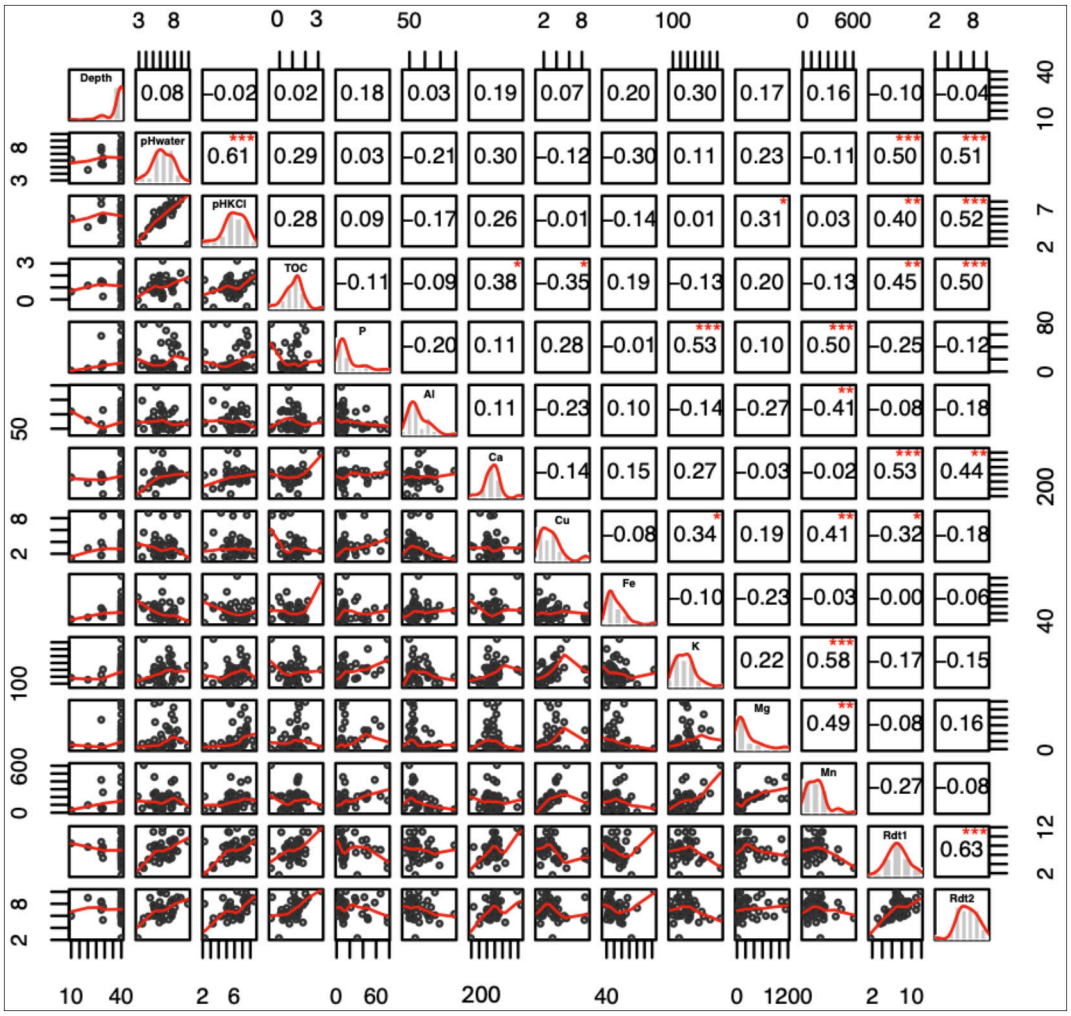

Fig. 12. Correlation and distribution matrix illustrating relationships between soil properties and grain maize yield for the 2022–2023 (Rdt1) and 2023–2024 (Rdt2) growing seasons. Pearson correlation coefficients (r) are represented by a colour gradient indicating both magnitude and sign (positive or negative). Asterisks denote levels of statistical significance (* $p < 0.05$; ** $p < 0.01$; *** $p < 0.001$).

spatially coherent results than kriging, Inverse Distance Weighted (IDW), Simple Spline, and Natural **Neighbor** interpolation. These alternative methods, which do not explicitly account for spatial discontinuities or physical barriers, tended to over-smooth spatial patterns or generate artefacts in areas characterized by abrupt changes in soil properties, leading to higher RMSE values, increased bias, and, in some cases, a pronounced "bull's-eye" effect (Metahni et al., **2019**), When compared with the Spline With Barriers approach.

The Spline With Barriers model consistently exhibited lower RMSE values, indicating greater predictive accuracy for unsampled locations (Smith and Smith, **2007**). In addition, bias values were close to zero, reflecting a balanced distribution of prediction errors and a reduced tendency toward systematic over- or underestimation (Harwell, **2018**). This method is particularly effective because it explicitly integrates spatial barriers or constraints, such as natural boundaries or abrupt landscape features, which strongly influence the spatial distribution of soil properties (Childs, **2004**).

The relevance of this approach has also been demonstrated in previous studies. Stupen et al. (**2022**) successfully applied the Spline With Barriers model to the construction of digital terrain models, showing that it effectively preserved local extremes and spatial discontinuities, thereby improving the representation of complex topographic patterns. In the present study, this capability proved essential for capturing the strong spatial heterogeneity induced by plinthite occurrence, subsoiling operations, and the uneven distribution of termite mound materials across the study area.

4.2. *Assessment of the effectiveness of subsoiling on soil depth*

The spatial distribution of soil thickness after subsoiling reveals pronounced spatial variability across the entire study area. This heterogeneity highlights critical zones where soil thickness remains below 9 cm, with plinthite locally exposed at the surface. Such conditions clearly indicate the limited effectiveness of the first subsoiling pass in these areas and support the need for additional subsoiling operations to further increase soil depth and, consequently, maximize the effective rooting volume available to crops.

Several studies have demonstrated that properly implemented subsoiling can substantially improve soil functionality, including soil structure, porosity, and rooting conditions (Cote and Dupuis, **1980**; Grevers and De Jong, **1993**; Steppuhn et al., **1995**; Wang et al., **2023a**). However, the effectiveness of subsoiling strongly depends on soil characteristics and the type of equipment used, as emphasized by Caban et al. (**2024**); Wang et al. (**2024b**) also showed that non-uniform loosening can limit the agronomic benefits of the practice. In the present study, shallow soils are mainly concentrated in the central part of the study area, where the restricted trophic volume severely constrains root development, thereby reducing plant access to both water and nutrients.

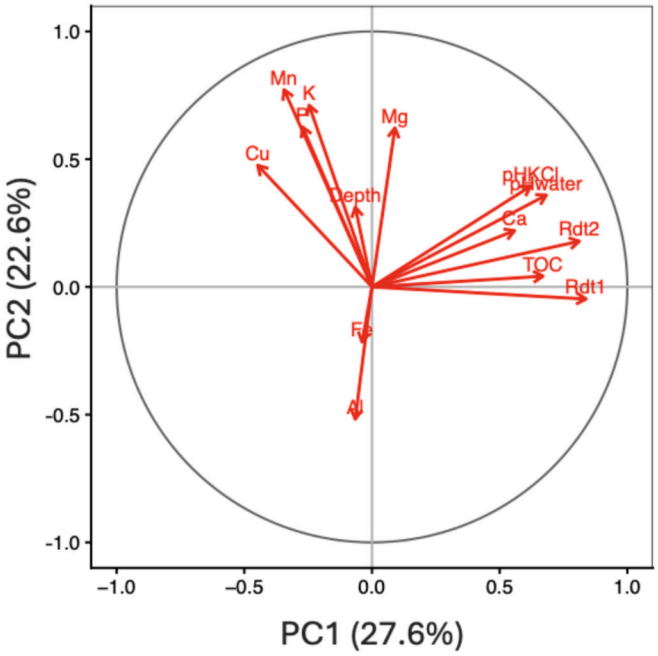

Fig. 13. Principal component analysis (PCA) correlation circle illustrating the relationships between soil properties and maize grain yields (Rdt1 and Rdt2). The first two principal components explain 50.2% of the total variance (PC1 = 27.6%, PC2 = 22.6%). Variables positioned close to each other indicate positive correlations, whereas variables oriented in opposite directions indicate negative relationships.

The presence of plinthite represents a major pedological constraint to soil depth management, as it forms a physical barrier that restricts root penetration and water movement (Brogowski and Kwasowski, **2012**; Daniels et al., **1978**; de Moraes et al., **2006**; Jien et al., **2010**; Wang et al., **2020**; WRB-IUSS, **2015**). Under such conditions, at least one additional subsoiling pass appears essential to ensure sufficient soil depth for sustainable crop production.

When correctly applied, subsoiling has been widely recognized as an effective management practice for improving soil structure, enhancing aeration, promoting deeper root penetration, and increasing access to water and nutrients (Alonso et al., **2023**; Huang et al., **2024a**; Huang et al., **2024b**; Li et al., **2024**; Šarauskis et al., **2024**; Wang et al., **2023a**; Wang et al., **2023b**; Wu et al., **2024**; Xie et al., **2024**). In plinthitic environments similar to those of the present study, Boubacar et al. (**2017**) reported a 72% reduction in annual runoff in subsoiled plots compared to untreated controls on Plinthosols in Tondi Kiboro (Niger), illustrating the hydrological benefits of effective subsoiling. Beyond mechanical interventions, traditional soil management practices in West Africa also aim to maintain or increase effective soil depth in Plinthosols. For instance, Asiamah and Dwomo (**2010**) reported that farmers in Burkina Faso and Ghana maintain arable soil thickness through the construction of stone dikes, while in Mali and Senegal, the Zaï technique is used to enhance soil depth and fertility. These practices underscore the central role of soil depth management in overcoming the limitations imposed by plinthite, and they support the relevance of subsoiling as a complementary or alternative strategy under mechanized farming conditions.

4.3. Spatial variation in soil chemical properties

The spatial distribution of soil chemical properties in the 0–10 cm layer after mechanical subsoiling and amendment with termite mound materials reveals marked spatial heterogeneity, reflecting both intrinsic soil variability and contrasts in the incorporation of amendments across the study area. Soil pH measured in KCl exhibits values below 4.1 and above 7.8, distributed throughout the site, indicating complex and spatially structured pedochemical dynamics. Blocks located in the northern part of the site, close to the river, display more pronounced soil acidification, likely associated with enhanced leaching of base cations and hydrological accumulation of H^+ ions (De Dapper and Malaisse, **1979**). This observation corroborates the findings of Sanchez (**2018**), who reported that intense leaching promotes soil acidification and favours plinthite formation.

Soil acidity in these areas is further exacerbated by the high iron oxide (Fe_2O_3) content typical of plinthitic soils, which enhances proton buffering and limits base saturation (Brogowski and Kwasowski, **2012**; Eze et al., **2010**; Jones et al., **2013**; Legros, **2013**; WRB-IUSS, **2015**). In contrast, central areas of the study area exhibit pH values above 5.5, corresponding to neutral to slightly alkaline soil conditions. This pattern is likely explained by the more effective incorporation of calcium-rich termite mound materials, often containing calcium carbonate ($CaCO_3$) (Adhikary et al., **2016**; Jouquet et al., **2015**; Li et al., **2017**; Mujinya et al., **2013**; Padonou et al., **2020**; Rajeev and Sanjeev, **2011**). Through dissociation into Ca^{2+} and CO_3^{2-}, carbonate ions neutralize H^+, thereby increasing soil pH (Ma et al., **2024**). This mechanism supports the conclusions of Asiamah and Dwomo (**2010**), who demonstrated that calcium amendments can substantially improve the productivity of Plinthosols by correcting soil acidity. However, some localized areas show pH values in water exceeding 8.7, indicating excessive alkalinity, which may limit micronutrient availability (Jobbágy et al., **2017**). Total organic carbon (TOC) contents range from less than 0.4% to more than 2.5%, reflecting the overall organic matter poverty typical of plinthitic and ferralitic soils (Brogowski and Kwasowski, **2012**; Dos Santos et al., **2018**; Fritsch et al., **2007**; Giorgis et al., **2014**; Kumar et al., **2018**). In this regard, Hounkpatin et al. (**2018**) reported a loss of 24 t C ha^{-1} over 29 years on a Plinthosol in Burkina Faso, highlighting the long-term vulnerability of these soils.

A slight increase in TOC near the river likely reflects higher biomass production and regular inputs of plant residues from floodplain environments (Wang et al., **2024c**). Nevertheless, TOC levels remain modest overall, suggesting that the positive effects of termite mound amendments are either spatially limited or partially offset by rapid organic matter mineralization, leaching, and poor residue incorporation(Chizen et al., **2024**).

Nutrient distributions also exhibit strong spatial variability. Available phosphorus remains globally low (from <5.1 to >145.5 mg kg^{-1}), with localized peaks in blocks B7 and B10. This pattern is consistent with strong P fixation by iron and aluminium oxides commonly found in plinthitic soils (Delfim et al., **2024**; Gotz et al., **2024**; Laurent and Brossard, **1991**; Rotta et al., **2015**; Sanchez, **2018**; Useni et al., **2014**). Elevated P concentrations in specific blocks may reflect residual effects of previous phosphate fertilizer applications, indicating a localized anthropogenic contribution.

Calcium concentrations locally exceed 18,267.7 mg kg^{-1}, confirming the high calcium content of termite mound materials (Adhikary et al., **2016**; Mujinya et al., **2013**). While beneficial for correcting soil acidity, such high Ca levels require careful management to avoid nutrient imbalances and antagonistic effects (Lehto, **1994**; Sediqui et al., **2024**). Aluminium (<44.4 to >293.4 mg kg^{-1}) and iron (up to >351.7 mg kg^{-1}) are abundant, which is characteristic of plinthitic materials (Davies, **1997**; Ngon Ngon et al., **2009**; Roquin et al., **1990**; Soil Survey Staff, **2014**), but these elements may reduce phosphorus availability and exert toxic effects on plants at high concentrations (Bell et al., **2024**; Fang et al., **2024**; Shi et al., **2024**). Copper concentrations can exceed 25.8 mg kg^{-1}, reflecting the copper-rich geochemical background of the Lubumbashi region (Bogaert et al., **2019**). These concentrations may be further redistributed by termite-driven bioturbation (Jouquet et al., **2020**). Manganese (<4.4 to >669.4 mg kg^{-1}) and magnesium (<238.8 to >2987.4 mg kg^{-1}) show marked spatial variability, largely controlled by the degree of amendment incorporation and soil hydrological conditions (Lahori et al., **2024**; Widdowson, **2009**; Woś et al., **2024**; Xu et al., **2024**). Finally, potassium ranges from <130.2 to >942.0 mg kg^{-1},

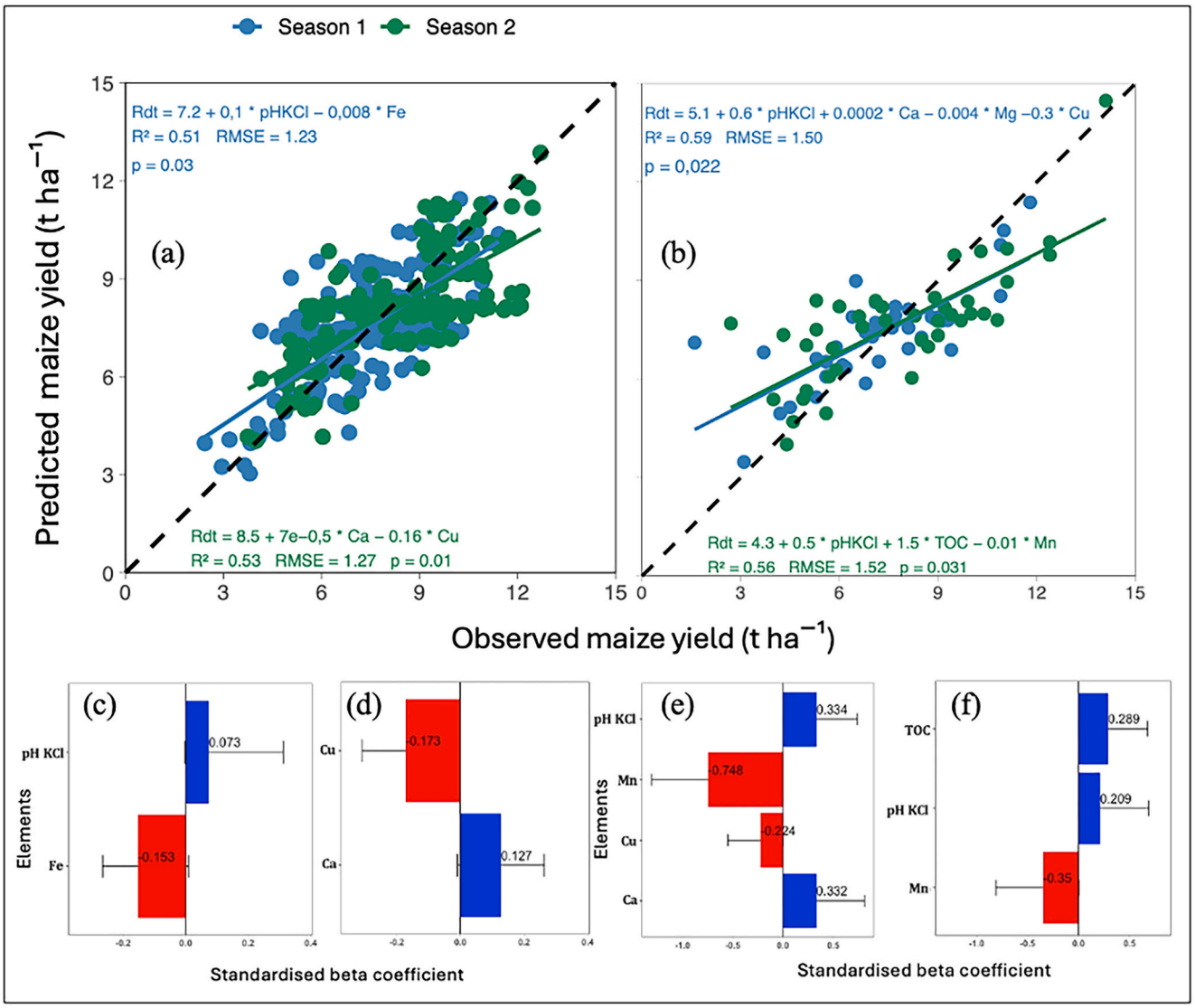

Fig. 14. Relationships between observed and predicted grain maize yields obtained from stepwise linear regression models based on yield map pixel values (a) and field-measured yields (b) for the 2022–2023 and 2023–2024 growing seasons. Bar charts display the standardized beta coefficients (±95% confidence intervals) of the explanatory variables included in the models: (c) and (d) correspond to pixel-based models, whereas (e) and (f) correspond to models based on field-measured yields for the two seasons, respectively. Solid lines represent fitted regression relationships, and the dashed line represents the 1:1 reference line.

with lower concentrations observed near the river, likely due to topographically-driven leaching toward low-lying areas (Akhatov et al., 2024; Alexandre, 2002; De Dapper and Malaisse, 1979; Nascimento et al., 2024).

4.4. *Physicochemical and hydric characterization in soil profiles*

The results obtained after mechanical subsoiling and amendment with termite mound materials reveal a high degree of heterogeneity in the physical, chemical, and hydraulic properties of soils, closely linked to the variability of soil profiles and horizon differentiation. Soil pH measured in water ranges from 5.7 to 8.4, indicating slightly acidic to slightly alkaline conditions that are generally favourable for nutrient availability, whereas the lower pH measured in KCl (4.2 to 7.6) reflects complex chemical interactions within the soil exchange complex, influenced by ionic exchanges between soil particles and amendments (Adhikary et al., 2016; Jouquet et al., 2015; Li et al., 2017; Padonou et al., 2020; Rajeev and Sanjeev, 2011; WRB-IUSS, 2015). Total organic carbon (TOC) contents remain generally low, but locally exceed 2% in surface horizons, highlighting the contribution of organic matter from termite mound materials. This variability is typical of ferralitic and plinthitic soils, which are characterized by a limited capacity to stabilize organic matter, often associated with coarse textures, weak aggregation, and rapid mineralization (Kasongo, 2008; Sanchez, 2018). Available phosphorus contents are also generally low, likely due to strong fixation by iron and aluminium oxides associated with plinthite (Delfim et al., 2024; Gotz et al., 2024; Laurent and Brossard, 1991; Rotta et al., 2015; Tshibangu et al., 2022). Nevertheless, a high surface value of 154.8 mg kg^{-1} observed in block B10 suggests a residual effect of previous phosphorus inputs. Calcium reaches exceptionally high concentrations in surface horizons, confirming the calcium-rich nature of termite mound materials (Adhikary et al., 2016; Ekundayo and Aghatise, 1997; Harit et al., 2017; Jouquet et al., 2015; Mujinya et al., 2013). While beneficial for correcting soil acidity, such high Ca levels require careful management to avoid excessive alkalinization and nutrient imbalances (Lehto, 1994; Sediqui et al., 2024). Potassium and magnesium show overall improvements in chemical fertility, whereas iron, manganese, and aluminium exhibit high and spatially heterogeneous concentrations, characteristic of Plinthosols formed through long-term Fe, Al, and Mn accumulation processes (Carvalho et al., 1991; Daniels et al., 1978;

Eswaran et al., 1990; Nahon, 2003; Roquin et al., 1990). According to WRB-IUSS (2007), aluminium concentrations in Plinthosols can reach 100 g kg^{-1} and exceed 300 g kg^{-1} in petroplinthite, while iron contents can also exceed 100 g kg^{-1}, underscoring the intensity of these pedogenic processes.

Particle-size analysis reveals a clear vertical textural differentiation, typical of plinthitic soils, characterized by an increase in clay content with depth, indicative of illuviation processes (Fritsch et al., 2007; Nahon, 2003). Such vertical differentiation is common in highly weathered tropical soils and results from the downward translocation of fine particles from surface to subsurface horizons, a process often associated with plinthite formation (Asiamah and Dwomo, 2010; Santos et al., 2023; WRB, 2022; Yoboue et al., 2019). Surface horizons exhibit higher sand contents in some blocks (B1, B6, B8, and B10), reflecting erosion and leaching of cultivated layers (Kasongo, 2008; Sanchez, 2018). In contrast, subsurface horizons (AB, Bs, and Bcs) show higher clay contents (up to 44%), resulting in denser soil structures that restrict permeability and root penetration (Brogowski and Kwasowski, 2012; de Moraes et al., 2006).

These findings emphasize the central role of plinthite in controlling textural differentiation and imposing physical constraints within soil profiles. The incorporation of termite mound materials, which are finer-textured and enriched in base cations (Jouquet et al., 2015; Mujinya et al., 2010), can improve the structure and fertility of surface horizons. However, their effectiveness remains strongly dependent on appropriate profile management, particularly through subsoiling to disrupt compacted layers and enhance amendment incorporation.

From a physical perspective, bulk density is lower in surface horizons (1.17–1.53 g cm^{-3}) and increases toward compact plinthic horizons, reaching values of up to 1.92 g cm^{-3}, reflecting a surface structural improvement linked to termite mound amendments, while strong physical constraints persist at depth. These values remain lower than those reported by the FAO (2001) for petroplinthite (2.5–3.6 g cm^{-3}), and surface bulk densities are consistent with the ranges reported by Brady and Weil (2008) for Ap horizons (1.2-1.5 g cm^{-3}).

Saturated hydraulic conductivity (Ksat) shows strong vertical variability, with high values in surface horizons (up to 7780 mm day^{-1} in B1 and B3, and 1810 mm day^{-1} in B9) and much lower values in deeper horizons (e.g., 63.9 mm day^{-1} in the Bs horizon of profile B5). This pattern indicates restricted infiltration and water movement at depth due to plinthite, consistent with findings by de Moraes et al. (2006). Plinthite, characterized by low porosity and irreversible hardening, therefore acts as a major barrier to both water circulation and root penetration (Brogowski and Kwasowski, 2012; Jacobs et al., 2002; Liu et al., 2020; Sarkar and Bandyopadhyay, 2018; Stiles et al., 2001; Wildemeersch et al., 2015; Yaro et al., 2006). In this context, Wu et al. (2010) reported 41.8% improvement in basalt permeability following polymer application, highlighting the difficulty of permanently alleviating such physical constraints.

Finally, soil water content at field capacity (DUL) is higher in surface horizons (0.257–0.302 *v*/v) and decreases with depth (0.115–0.154 v/v), while the wilting point (LL) is lower at the surface (0.094–0.159 v/v) but relatively high in plinthic horizons, reaching values of up to 0.226 v/v. This configuration results in greater plant-available water in surface layers, thereby promoting improved crop water supply. The enhanced surface water retention reflects the positive influence of termite mound materials on mesopore abundance and connectivity (Feiza et al., 2015; Pessoa et al., 2024). Mesopores preferentially retain water at field capacity, whereas micropores retain water more strongly, explaining the elevated LL values observed in deeper horizons (Dalmago et al., 2009). Several studies have similarly demonstrated that subsoiling combined with organo-mineral amendments improves soil hydraulic properties and water availability in surface horizons (Alonso et al., 2023; Liu et al., 2024; Ramadhan and Alfaris, 2023; Wang et al., 2024a; Wu et al., 2024).

4.5. Spatial variation in grain maize yield

The spatial distribution of grain maize yields reveals a wide range of productivity, with values varying from less than 2.3 to more than 11.1 t ha^{-1}, depending on location within the study perimeter. This marked spatial heterogeneity can be attributed to local differences in soil physicochemical properties, soil water availability, and the variable effectiveness of subsoiling operations across the site. Nevertheless, the yields obtained in this study are substantially higher than the regional average of 0.77 t ha^{-1} reported for smallholder farmers in 2023 according to FAOSTAT (**https://www.fao.org/faostat/fr/#data**, accessed 10 February 2025), highlighting the strong positive impact of subsoiling combined with amendments using termite mound materials.

Numerous studies support the beneficial effects of subsoiling on maize productivity, including those reported by Ramadhan and Alfaris (2023) in Iraq, as well as Wang et al. (2024a), and Li et al. (2024) in China. In addition, several studies have demonstrated the agronomic advantages of termite mound soil amendments, owing to their enriching chemical composition and contribution to improved soil fertility (de Lima et al., 2018; Enagbonma and Babalola, 2019; Eze et al., 2019; Jouquet et al., 2015; Kaschuk et al., 2006; Mujinya et al., 2013; Padonou et al., 2020; Rajeev and Sanjeev, 2011), thereby contributing to increased crop yields.

During the first growing season, however, blocks B8 and B10 exhibited consistently lower yields, likely due to persistent soil limitations, including shallow effective soil depth, residual compaction, and reduced nutrient retention capacity, despite the applied amendments. According to WRB-IUSS (2015), the limited thickness of Plinthosols restricts both water percolation and root penetration, thereby constraining crop productivity. In contrast, low-lying areas near the river consistently recorded higher yields, probably due to improved water availability and higher organic matter inputs, which tend to increase closer to riparian zones. Several studies have emphasized that soils enriched in organic matter optimize crop yields by improving nutrient supply and soil structure (Obalum et al., 2017; Paul, 2016; Sanchez, 2018; Voltr et al., 2021). Moreover, Pessoa et al. (2024) showed that adequate soil water availability enhances crop growth, nutrient uptake, resistance to water stress, and ultimately overall agricultural productivity.

During the second growing season, yields exhibited a generalized increase across the study area, with an average gain of approximately 1 t ha^{-1}. This improvement can be attributed to the cumulative and delayed effects of subsoiling and soil amendments, which begin to manifest more clearly over time, even in previously low-yielding zones such as parts of blocks B8 and B10. Although the magnitude of the increase remains moderate, this trend underscores the importance of long-term soil management strategies for progressively enhancing yield potential in initially constrained plinthitic environments. Supporting this interpretation, Wildemeersch et al. (2015) reported a significant long-term increase in millet yields in Nigeria, reaching 0.7 ± 0.2 Mg ha^{-1} on marginal Plinthosols following the implementation of soil and water conservation practices.

4.6. Optimization of grain maize yield: regression models and analysis

Correlation analyses revealed a positive association between maize grain yield and soil pH, calcium (Ca), and total organic carbon (TOC), confirming the central role of soil acidity neutralization and improved nutrient availability in sustaining productivity in tropical agroecosystems (Sanchez, 2018). In contrast, elevated copper (Cu) concentrations, particularly during the first growing season, were negatively associated with yield, which is consistent with the phytotoxic effects of Cu in metal-enriched soils (Mubemba et al., 2017; Yruela, 2009). These relationships were further corroborated by principal component analysis (PCA). The first axis (PC1, explaining 27.6% of the total variance) represents an edaphic fertility gradient dominated by pH, Ca, and TOC,

along which maize yields from both seasons (Rdt1 and Rdt2) were positively aligned, whereas Cu was oriented in the opposite direction, indicating its limiting effect on crop production. The second axis (PC2, 23.6% of the variance), contrasting Mn–K–P–Mg–depth with Fe—Al, accounted for a smaller proportion of yield variability. Nevertheless, second-season yield (Rdt2) exhibited a negative association with Mn, highlighting the potentially restrictive role of excessive Mn on the uptake of other essential cations (Lahori et al., **2024**; Sanchez, **2018**; Xu et al., **2024**).

These multivariate relationships were confirmed and quantitatively refined by stepwise linear regression models, which emphasized the dominant influence of specific edaphic parameters on yield variability. During the first growing season, the regression model showed a statistically significant effect ($p = 0.03$), with soil pH measured in KCl and iron (Fe) identified as key explanatory variables. Standardized beta coefficients indicated a negative association between Fe and grain maize yield. This relationship can be explained by the acidifying effect of iron oxides (Fe_2O_3), which enhance soil acidity and may impair crop growth (Sanchez, **2018**). Moreover, at high concentrations, Fe can reduce phosphorus availability by forming insoluble compounds such as iron phosphate ($FePO_4$) (Agbenin, **2003**; Barrow et al., **2018**; de Campos et al., **2018**; Rosolem et al., **2024**). Consequently, high total P contents do not necessarily translate into plant-available P, thereby limiting nutrient uptake and crop performance. In addition, excessive iron may induce nutritional imbalances and toxic effects, further constraining yield potential (da Silva et al., **2024**; Han et al., **2024**; Tsamos et al., **2024**). Conversely, an increase in pH KCl was positively associated with grain yield, indicating that reducing soil acidity enhances nutrient availability and crop physiological performance (Sanchez, **2018**; WRB-IUSS, **2007**).

During the second growing season, the regression model remained statistically significant ($p = 0.01$) and identified calcium (Ca) and copper (Cu) as the main determinants of grain maize yield. Elevated Cu concentrations were again associated with yield reductions. Although Cu is an essential micronutrient at low concentrations, excessive levels can become toxic, inhibiting root development and disrupting plant nutrition. In the Lubumbashi region, Mpundu et al. (**2013**) reported stunted growth and high Cu bioaccumulation in vegetable crops, confirming the agronomic risks associated with Cu enrichment.

In contrast, higher Ca concentrations were positively correlated with yield, reflecting the beneficial role of Ca in improving soil structure, enhancing aeration and permeability, and facilitating nutrient uptake by plant roots (Bakker, **2018**; Meriño-Gergichevich et al., **2010**; Mubemba et al., **2014**; Mujinya et al., **2013**; Olego et al., **2021**). For instance, Anikwe et al. (**2016**) reported cassava yields of 9.5 Mg ha^{-1} on limestone-amended plots, compared to 6.1 Mg ha^{-1} on untreated Ultisols in Nigeria, illustrating the agronomic benefits of Ca-based amendments.

Regression models based on field-measured grain maize yields further highlighted season-dependent controls on productivity. During the first season, soil pH, Mn, Cu, and Ca were identified as significant predictors ($p = 0.02$). Standardized beta coefficients showed that high Mn and Cu concentrations were negatively associated with yield, likely due to nutrient antagonisms and toxicity effects. Excess Mn can disrupt soil nutrient balance by inhibiting the uptake of other essential cations such as Ca and K (Sanchez, **2018**), while excessive Cu is known to damage root systems and impair plant metabolism (Mubemba et al., **2017**; Yruela, **2009**).

In contrast, increasing soil pH and Ca levels exerted a strong positive influence on yield, with increases of 0.334 and 0.332 standard deviations, respectively. This finding underscores the critical importance of acidity management for optimizing nutrient availability, as emphasized by Sanchez (**2018**) and WRB-IUSS (**2015**), who reported that optimal pH conditions enhance the uptake of essential nutrients.

During the second season, soil pH, Mn, and TOC emerged as the main controlling factors ($p = 0.03$). The negative effect of Mn on yield again supports the hypothesis that excessive Mn concentrations induce nutritional imbalances (Lahori et al., **2024**; Woś et al., **2024**; Xu et al., **2024**). Conversely, higher soil pH and organic carbon contents positively affected yield, consistent with numerous studies demonstrating that soil organic matter improves water retention, nutrient storage, and overall soil resilience, thereby enhancing crop growth (Garcia et al., **2024**; Malik et al., **2024**; Naeem et al., **2024**; Obalum et al., **2017**; Paul, **2016**; Voltr et al., **2021**; Zhang et al., **2024**).

Although all regression models exhibited coefficients of determination exceeding 50%, clear differences emerged depending on the source of yield data. Models based on pixel values extracted from yield maps showed lower R^2 values, likely due to the interpolated nature of these data, which may not fully capture fine-scale spatial variability. In contrast, models calibrated with field-measured yields achieved higher R^2 values, indicating greater predictive accuracy and robustness. This observation aligns with Akinwande et al. (**2015**), who emphasized the importance of high-quality input data and rigorous validation procedures. To further enhance model performance, the integration of additional environmental and management variables (e.g., microtopography, soil moisture dynamics, and historical management practices) remains a relevant perspective.

5. Conclusion

This study demonstrates the significant and combined effects of mechanical subsoiling and termite mound material amendments on the fertility of Plinthosols and grain maize productivity in the Lubumbashi region. The results show that areas requiring secondary subsoiling, where soil thickness remains below 9 cm, present persistent physical constraints to crop growth, whereas blocks exhibiting soil thicknesses greater than 73 cm offer substantially higher potential for agricultural production by increasing the effective rooting volume.

The analysis of soil physicochemical properties revealed marked spatial variability in soil pH, total organic carbon (TOC), and essential nutrients, including phosphorus, calcium, potassium, and magnesium. In contrast, high concentrations of aluminium, iron, and copper were observed, displaying heterogeneous spatial distributions, with copper showing a relatively uniform background pattern consistent with the regional geochemical context. From a hydrodynamic perspective, soils exhibited low saturated hydraulic conductivity at depth, reflecting restricted vertical water movement imposed by plinthite, whereas surface water retention was improved, indicating enhanced porosity and increased plant-available water following amendment incorporation.

Grain maize yields showed strong spatial heterogeneity, ranging from less than 2.3 to more than 11.1 t ha^{-1}, with a notable increase in mean yield from 7.1 to 8.2 t ha^{-1} between the first and second growing seasons. Stepwise regression models based on pixel values extracted from yield maps indicated that high iron and copper concentrations negatively affect yield, while higher soil pH and calcium availability exert a positive influence. In parallel, regression models based on field-measured yields, which proved to be more robust and reliable, confirmed that soil pH, calcium, and total organic carbon are the main positive determinants of maize yield, whereas excessive concentrations of copper, iron, and manganese are associated with yield reductions, likely due to nutritional imbalances and indirect effects on soil acidity. Although all models exhibited coefficients of determination (R^2) exceeding 0.50, field-based models provided greater explanatory power than map-derived pixel-based models.

Overall, these findings emphasize that improving soil chemical fertility through pH regulation, calcium enrichment, and organic matter enhancement is central to increasing maize productivity and ensuring the sustainable management of Plinthosols. The combined use of targeted subsoiling and locally available termite mound materials emerges as a promising and context-adapted strategy for overcoming the physical and chemical constraints of plinthitic soils in the southern Democratic Republic of the Congo and similar tropical environments.

However, the lack of prior chemical and mineralogical characterization of termite mound materials limits the precise assessment of their specific contribution to the observed improvements in soil properties and maize yield; future studies incorporating such characterization would allow a more accurate quantification of their effects.

CRediT authorship contribution statement

John Banza Mukalay: Writing – review & editing, Writing – original draft, Visualization, Validation, Supervision, Software, Methodology, Investigation, Formal analysis, Data curation, Conceptualization. **Jeroen Meersmans:** Writing – review & editing, Visualization, Validation, Resources, Methodology, Formal analysis. **Joost Wellens:** Writing – review & editing, Visualization, Validation, Resources. **Yannick Useni Sikuzani:** Writing – review & editing, Visualization, Validation, Software, Resources. **Emery Kasongo Lenge Mukonzo:** Writing – review & editing, Visualization, Validation, Software, Methodology, Investigation, Formal analysis, Conceptualization. **Gilles Colinet:** Writing – review & editing, Visualization, Validation, Supervision, Software, Resources, Project administration, Methodology, Investigation, Funding acquisition, Formal analysis, Conceptualization.

Funding statement

This research was funded by Académie de Recherche et d'Enseignement Supérieur (ARES-CCD) through the B-Mob grant, as well as by the PACODEL Impulse grant, Belgium.

Declaration of competing interest

The authors declare that they have no known competing financial interests or personal relationships that could have appeared to influence the work reported in this paper.

Acknowledgments

The authors gratefully acknowledge the Académie de Recherche et d'Enseignement Supérieur (ARES-CCD), Belgium, for funding this research. They also extend their sincere thanks to the management of FarmCo MMG, in particular Eng. Deo Mwamba and Eng. Célestin Nkulu, for granting access to the study site and for their support throughout the research activities. The authors also gratefully acknowledge the laboratory technicians at Gembloux Agro-Bio Tech—Emilie Marit, Pauline Biron, Aurore Houtart, Catherine Paquet, Jean-Charles Bergen, Raphaël Tarantino, and Stéphane Becquevort—for their valuable technical assistance with soil physicochemical and hydrodynamic analyses.

Appendix A. Supplementary data

Supplementary data to this article can be found online at https://doi.org/10.1016/j.geodrs.2026.e01066.

Data availability

Data will be made available on request.

References

Adeyanju, D., Mburu, J., Gituro, W., Chumo, C., Mignouna, D., Ogunniyi, A., Akomolafe, J.K., Ejima, J., 2023. Assessing food security among young farmers in Africa: evidence from Kenya, Nigeria, and Uganda. Agric. Food Econ. 11. https://doi.org/10.1186/s40100-023-00246-x.

Adhikary, N., Erens, H., Weemaels, L., Deweer, E., Mees, F., Mujinya, B.B., Baert, G., Boeckx, P., Van Ranst, E., 2016. Effects of spreading out termite mound material on Ferralsol fertility, Katanga, D.R. Congo Commun Soil Sci Plant Anal 47, 1089–1100. https://doi.org/10.1080/00103624.2016.1166237.

Agbenin, J.O., 2003. Extractable Iron and aluminum effects on phosphate sorption in a savanna Alfisol. Soil Sci. Soc. Am. J. 67, 589–595. https://doi.org/10.2136/sssaj2003.5890.

Akhatov, A., Nurmatova, V., Usmonova, B., 2024. The influence of slope exposure, profile depth and Erosion processes on changes in the content of potassium, phosphorus and humus in Brown soils of mountain pastures of Uzbekistan. Yuzuncu Yil Univ. J. Agricult. Sci. 34, 224–234. https://doi.org/10.29133/yyutbd.1393784.

Akinwande, M.O., Dikko, H.G., Samson, A., 2015. Variance inflation factor: as a condition for the inclusion of suppressor variable(s) in regression analysis. Open J. Stat. 05, 754–767. https://doi.org/10.4236/ojs.2015.57075.

Alexandre, J., 2002. Les cuirasses lateritiques et autres formations ferriguneuses tropicals exemple du Haut Katanga Méridional. Mus. roy. Afr. centr., Tervuren, Ann. Sc. Géol 129.

Alonso, M., López, G., Grajales, M., 2023. Mejoramiento de las propiedades hidráulicas del suelo en el cultivo de soya mediante el subsuelo. Rev Mex De Cienc Agric 78–89.

Anikwe, M.A.N., Eze, J.C., Ibudialo, A.N., 2016. Influence of lime and gypsum application on soil properties and yield of cassava (Manihot esculenta Crantz.) in a degraded Ultisol in Agbani. Enugu Southeastern Nigeria Soil Tillage Res 158, 32–38. https://doi.org/10.1016/j.still.2015.10.011.

Asiamah, R.D., Dwomo, O., 2010. Ethno-management of plinthic and ironpan soils in the savanna regions of West Africa. Ghana J. Agricult. Sci. 42, 25–29. https://doi.org/10.4314/gjas.v42i1-2.60641.

Assani, A.A., 1999. Analyse de la variabilité temporelle des précipitations (1916-1996) à Lubumbashi (Congo-Kinshasa) en relation avec certains indicateurs de la circulation atmosphériques (oscillation austral) et océaniques (El Niño/La Niña). Sécheresse 10, 245–252.

Bakker, M., 2018. Effet des amendements calciques sur les racines fines de chêne (*Quercus petraea* et robur): conséquences des changements dans la rhizosphère. Université Henri Poincaré - Nancy 1.

Banza, M.J., Mwamba, K.F., Esoma, E.B., Meta, T.M., Mayamba, M.G., Kasongo, L.M.E., 2019. Evaluation de la réponse du maïs (Zea mays L.) installé entre les haies de Tithonia diversifolia à Lubumbashi, R.D. Congo. J. Appl. Biosci. 134, 13643. https://doi.org/10.4314/jab.v134i1.3.

Barrow, N.J., Debnath, A., Sen, A., 2018. Mechanisms by which citric acid increases phosphate availability. Plant Soil 423, 193–204. https://doi.org/10.1007/s11104-017-3490-8.

Baumgartner, S., Bauters, M., Barthel, M., Drake, T.W., Ntaboba, L.C., Bazirake, B.M., Six, J., Boeckx, P., Van Oost, K., 2021. Stable isotope signatures of soil nitrogen on an environmental-geomorphic gradient within the Congo Basin. Soil 7, 83–94. https://doi.org/10.5194/soil-7-83-2021.

Bell, L.E., Moir, J.L., Black, A.D., 2024. The effects of soil acidity and Aluminium on the root systems and shoot growth of Lotus pedunculatus and Lupinus polyphyllus. Plants 13. https://doi.org/10.3390/plants13162268.

Beyene, S.D., 2023. The impact of food insecurity on health outcomes: empirical evidence from sub-Saharan African countries. BMC Public Health 23, 1–22. https://doi.org/10.1186/s12889-023-15244-3.

Bilong, P., 1992. Caractères des sols ferrallitiques à plinthite et à pétroplinthite développés sur roches acides dans la zone forestière du sud du Cameroun Comparaison avec les sols développés sur roches basiques, XXVII, pp. 203–224.

Bogaert, J., Colinet, G., Grégory, M., 2019. Anthropisation des paysages katangais. Presss Universitaire de Liège.

Boubacar, A., Malam Abdou, M., Ingatan Warzagan, A., Mamadou, I., Maiga, O.F., Moussa, I.B., 2017. Efficacité du sous-solage dans la restauration des sols sahéliens dégradés: étude expérimentale sur le site de Tondi Kiboro. Niger Afrique Sci. 13, 189–201.

Brady, N.C., Weil, R.R., 2008. The Nature and Properties of Soils, Fourteenth. ed.

Brogowski, Z., Kwasowski, W., 2012. Distribution of organic matter in the particle size fractions of lateritic soil (plinthosol). Soil Sci. Annu. 63, 9–15. https://doi.org/10.2478/v10230-012-0036-x.

Caban, J., Nieoczym, A., Krzywonos, L., 2024. Strength analysis of subsoiler tooth. Eng. Rural Develop. 23, 286–293. https://doi.org/10.22616/ERDev.2024.23.TF057.

Camacho, M.E., Mata, R., Barrantes-Víquez, M., Alvarado, A., 2021. Morphology and characteristics of eight Oxisols in contrasting landscapes of Costa Rica. Catena (Amst) 197, 104992. https://doi.org/10.1016/j.catena.2020.104992.

de Campos, M., Antonangelo, J.A., van der Zee, S.E.A.T.M., Alleoni, L.R.F., 2018. Degree of phosphate saturation in highly weathered tropical soils. Agric. Water Manag. 206, 135–146. https://doi.org/10.1016/j.agwat.2018.05.001.

Carvalho, I.G., Mestrinho, S.S.P., Fontes, V.M.S., Goel, O.P., de A. Souza, F., 1991. Geochemical evolution of laterites from two areas of the semiarid region in Bahia state, Brazil. J. Geochem. Explor. 40. https://doi.org/10.1016/0375-6742(91)90049-Z.

Childs, C., 2004. Interpolating surfaces in ArcGIS spatial analyst. ArcUser 32–35.

Chizen, C.J., Helgason, B.L., Weiseth, B., Dhillon, G.S., Baulch, H.M., Schoenau, J.J., Bedard-Haughn, A.K., 2024. Soil carbon dynamics in drained prairie pothole wetlands. Front Environ Sci 12, 1–18. https://doi.org/10.3389/fenvs.2024.1353802.

Coelho, M.R., Vidal-Torrado, P., 2000. Cério (Ce) em ferricretes nodulares desenvolvidos em solos da formação adamantina. Sci. Agric. 57, 329–336. https://doi.org/10.1590/S0103-90162000000200021.

Cooper, M.W., Brown, M.E., Niles, M.T., ElQadi, M.M., 2020. Text mining the food security literature reveals substantial spatial bias and thematic broadening over time. Glob Food Sec 26, 100392. https://doi.org/10.1016/j.gfs.2020.100392.

Cote, D., Dupuis, G., 1980. Effets du sous-solage et du labour profond sur les propriétés physiques du sol et le rendement de la luzerne et du maïs sur loam sableux Chaloupe. Can. J. Soil Sci. 353, 345–353. https://doi.org/10.1002/etc.5620160108.

Dalmago, G.A., Bergamaschi, H., Bergonci, J.I., Krüger, C.A.M.B., Comiran, F., Heckler, B.M.M., 2009. Retenção e disponibilidade de água às plantas, em solo sob plantio direto e preparo convencional. Revista Bras. Engenharia Agrícola e Ambiental 13, 855–864. https://doi.org/10.1590/s1415-43662009000700007.

Daniels, R.B., Perkins, H.F., Hajek, B.F., Gamble, E.E., 1978. Morphology of discontinuous phase Plinthite and criteria for its field identification in the southeastern United States. Soil Sci. Soc. Am. J. 42, 944–949.

Davies, B.E., 1997. Deficiencies and toxicities of trace elements and micronutrients in tropical soils: limitations of knowledge and future research needs. Environ. Toxicol. Chem. 16, 75–83. https://doi.org/10.1897/1551-5028(1997)016<0075:DATOTE>2.3.CO;2.

De Azevedo, J.R., Bueno, C.R.P., 2017. Potencialidades E Limitações Agrícolas De Solos Em Assentamento De Reforma Agrária No Município De Chapadinha-Ma. Sci. Agrár. 17, 1. https://doi.org/10.5380/rsa.v17i3.46841.

De Dapper, M., Malaisse, F., 1979. Rélations entre les différents stades d'érosion d'une cuirasse lateritique et la végétation sur le plateau de la Manika (Shaba, Zaïre). Geo Eco Trop 3, 99–117.

Delfim, J., Moreira, A., Moraes, L.A.C., Silva, J.F., Moreira, P.A.M., Lima Filho, O.F., 2024. Soil phosphorus availability impacts chickpea production and nutritional status in tropical soils. J. Soil Sci. Plant Nutr. 24, 3115–3130. https://doi.org/10.1007/s42729-024-01738-5.

Dos Santos, C.C., de Lima, Souza, Ferraz Junior, A., Oliveira Sá, S., Gutiérrez J., Andrés Muñoz, Braun, H., Sarrazin, M., Brossard, M., Desjardins, T., 2018. Soil carbon stock and Plinthosol fertility in smallholder land-use systems in the eastern Amazon, Brazil. Carbon Manag 9, 655–664. https://doi.org/10.1080/17583004.2018.1530026.

Dutta, S., Pal, R., Chakraborty, A., Chakrabarti, K., 2003. Influence of integrated plant nutrient supply system on soil quality restoration in a red and laterite soil. Arch. Agron. Soil Sci. 49, 631–637. https://doi.org/10.1080/03650340310001599722.

Ekundayo, E.O., Aghatise, V.O., 1997. Soil Properties of Termite Mounds under Different Land Use Types in a Typic Paleudult of Midwestern Nigeria 1–7.

Enagbonma, B.J., Babalola, O.O., 2019. Potentials of Termite Mound Soil bacteria in Ecosystem Engineering for Sustainable Agriculture 211–219.

Erens, H., Boudin, M., Mees, F., Mujinya, B.B., Baert, G., Strydonck, M. Van, Boeckx, P., Ranst, E. Van, 2015. The Age Oflarge Termite Mounds – Radiocarbon Dating of Macrotermes Falciger Mounds of the Miombo Woodland of Katanga. Palaeogeogr Palaeoclimatol Palaeoecol, DR Congo. https://doi.org/10.1016/j.palaeo.2015.06.017.

Eswaran, H., De Coninck, F., Varghese, T., 1990. Role of Plinthite and Related Forms in Soil Degradation 109–127. https://doi.org/10.1007/978-1-4612-3322-0_3.

Eze, P.N., Udeigwe, T.K., Stietiya, M.H., 2010. Distribution and potential source evaluation of heavy metals in prominent soils of Accra Plains, Ghana. Geoderma 156, 357–362. https://doi.org/10.1016/j.geoderma.2010.02.032.

Eze, P.N., Kokwe, A., Eze, J.U., 2019. Advances in nanoscale study of organomineral complexes of termite mounds and associated soils: a systematic review. Appl Environ Soil Sci 2020, 9. https://doi.org/10.1155/2020/8087273.

Fang, C., Wu, J., Liang, W., 2024. Systematic investigation of aluminum stress-related genes and their critical roles in plants. Int. J. Mol. Sci. 25, 1–21. https://doi.org/10.3390/ijms25169045.

FAO, 2001. Lecture Notes on the Major Soil of the World. Rome.

FAO, 2021. L'état de la sécurité alimentaire et de la nutrition dans le monde. Rome. https://doi.org/10.4060/cb5409fr.

Fauzi, A.I., Stoops, G., 2004. Reconstruction of a toposequence on volcanic material in the Honje Mountains, Ujung Kulon peninsula, West Java. Catena (Amst) 56, 45–66. https://doi.org/10.1016/j.catena.2003.10.004.

Feiza, V., Feizienė, D., Sinkevičienė, A., Bogužas, V., Putramentaitė, A., Lazauskas, S., Deveikytė, I., Seibutis, V., Steponavičienė, V., Pranaitienė, S., 2015. Soil water capacity, pore-size distribution and CO2 e-flux in different soils after long-term no-till management. Zemdirbyste-Agriculture 102, 3–14. https://doi.org/10.13080/z-a.2015.102.001.

Fritsch, E., Herbillon, A.J., Do Nascimento, N.R., Grimaldi, M., Melfi, A.J., 2007. From Plinthic Acrisols to Plinthosols and Gleysols: Iron and groundwater dynamics in the tertiary sediments of the upper Amazon basin. Eur. J. Soil Sci. 58, 989–1006. https://doi.org/10.1111/j.1365-2389.2006.00877.x.

Garcia, J., Mondragon-Becerra, M., Martinez, I., Nocco, M., Lazcano, C., 2024. Organic amendments alter urban soil microbiomes and improve crop quality. Appl. Soil Ecol. 204, 105731. https://doi.org/10.1016/j.apsoil.2024.105731.

Gebre, G.G., Rahut, D.B., 2021. Prevalence of household food insecurity in East Africa: linking food access with climate vulnerability. Clim. Risk Manag. 33, 100333. https://doi.org/10.1016/j.crm.2021.100333.

Giorgis, I., Bonetto, S., Giustetto, R., Lawane, A., Pantet, A., Rossetti, P., Thomassin, J.H., Vinai, R., 2014. The lateritic profile of Balkouin, Burkina Faso: geochemistry, mineralogy and genesis. J. Afr. Earth Sci. 90, 31–48. https://doi.org/10.1016/j.jafrearsci.2013.11.006.

Gotz, L.F., de Almeida, A.N.F., de Souza Nunes, R., Condron, L.M., Pavinato, P.S., 2024. Assessment of phosphorus use and availability by contrasting crop plants in a tropical soil. Biol. Fertil. Soils 60, 603–612. https://doi.org/10.1007/s00374-024-01833-w.

Grevers, M.C.J., De Jong, E., 1993. Soil structure and crop yield over a 5-year period following subsoiling Solonetzic and Chernozemic soils in Saskatchewan. Can. J. Soil Sci. 91, 81–91.

Han, X., Wu, H., Li, Q., Cai, W., Hu, S., 2024. Assessment of heavy metal accumulation and potential risks in surface sediment of estuary area: a case study of Dagu river. Mar. Environ. Res. 196, 106416. https://doi.org/10.1016/j.marenvres.2024.106416.

Harit, A., Moger, H., Louis, J., Selvaraj, D., Abbas, S., Sankaran, A., Pascal, S., 2017. Termites can have greater influence on soil properties through the construction of soil sheetings than the production of above-ground mounds. Insect. Soc. 64, 247–253. https://doi.org/10.1007/s00040-017-0541-3.

Harwell, M., 2018. A strategy for using bias and RMSE as outcomes in Monte Carlo studies in statistics. J. Mod. Appl. Stat. Methods 17. https://doi.org/10.22237/jmasm/1551907966.

Hounkpatin, K.O.L., Welp, G., Akponikpè, P.B.I., Rosendahl, I., Amelung, W., 2018. Carbon losses from prolonged arable cropping of Plinthosols in Southwest Burkina Faso. Soil Tillage Res. 175, 51–61. https://doi.org/10.1016/j.still.2017.08.014.

Huang, Chao, Liu, X., Gao, Y., Chen, H., Ma, S., Qin, A., Zhang, Y., Gao, Z., Song, Y., Sun, J., Liu, Z., 2024b. Response of Triticum Vulgare growth and nitrogen allocation to irrigation methods and regimes under subsoiling tillage. Agronomy 14. https://doi.org/10.3390/agronomy14040858.

Huang, Chengyi, Huang, H., Huang, S., Li, W., Zhang, K., Chen, Y., Yang, L., Luo, L., Deng, L., 2024a. Effects of straw returning on soil aggregates and its organic carbon and nitrogen retention under different mechanized tillage modes in typical hilly regions of Southwest China. Agronomy 14. https://doi.org/10.3390/agronomy14050928.

Jacobs, P.M., West, L.T., Shaw, J.N., 2002. Redoximorphic features as indicators of seasonal saturation, Lowndes County, Georgia. Soil Sci. Soc. Am. J. 66, 315–323. https://doi.org/10.2136/sssaj2002.3150.

Jien, S.-H., Hseu, Z.-Y., Chen, Z.-S., 2010. Hydropedological implications of Ferromanganiferous nodules in Rice-growing Plinthitic Ultisols under different moisture regimes. Soil Sci. Soc. Am. J. 74, 880–891. https://doi.org/10.2136/sssaj2009.0020.

Jobbágy, E.G., Tóth, T., Nosetto, M.D., Earman, S., 2017. On the fundamental causes of high environmental alkalinity (pH $\geq$ 9): an assessment of its drivers and global distribution. Land Degrad. Dev. 28, 1973–1981. https://doi.org/10.1002/ldr.2718.

Johnston, K., Hoef, J.M. Ver, Krivoruchko, K., Lucas, N., 2001. Using ArcGis Geostatical Analyst, 1st ed. ESRI Press, Redlands, CA, USA.

Jones, A., Breuning-Madsen, H., Brossard, M., Dampha, A., Deckers, J., Dewitte, O., Gallali, T., Hallett, S., Jones, R., Kilasara, M., Le Roux, P., Micheli, E., Montanarella, L., Spaargaren, O.T., Hiombiano, L., Van Ranst, E., Yemefack, M.R.Z., 2013. Soil Atlas of Africa. Publications Office of the European Union, Luxembourg, European Commission.

Jouquet, P., Guilleux, N., Ramesh, R., 2015. Influence of soil type on the properties of termite mound nests in southern India. Appl. Soil Ecol. 96, 282–287. https://doi.org/10.1016/j.apsoil.2015.08.010.

Jouquet, P., Jamoteau, F., Majumdar, S., Podwojewski, P., Nagabovanalli, P., Caner, L., Barboni, D., Meunier, J., 2020. The distribution of silicon in soil is in fluenced by termite bioturbation in south Indian forest soils. Geoderma 372, 114362. https://doi.org/10.1016/j.geoderma.2020.114362.

Kaschuk, G., Santos, J.C.P., Almeida, J.A., Sinhorati, D.C., Berton, J.F., 2006. Termite activity in relation to natural grassland soil attributes. Sci. Agric. 63, 583–588. https://doi.org/10.1590/S0103-90162006000600013.

Kasongo, L.M.E., 2008. Evaluation des terres à multiples échelles pour la détermination de l' impact de la gestion agricole sur la sécurité alimentaire au Katanga, R.D. Congo (Ph.D. Thesis). Université de Gent, Gent, Belgium. **https://biblio.ugent.be/publication/607168/file/18831** (verified 10 september 2025).

Kasongo, L.M.E., Banza, M.J., Meta, T.M., Mukoke, T.H., Kanyenga, F., Mayamba, M.G., Mwamba, K.F., Mazinga, K.M., 2019. Sensibilité de la culture pluviale du maïs (Zea mays L.) aux effets des épisodes secs sur un Ferralsol sous amendement humifère à Lubumbashi. J. Appl. Biosci. 140, 14316–14326.

Koppe, E., Rupollo, C.Z., de Queiroz, R., Uteau Puschmann, D., Peth, S., Reinert, D., 2021. Physical recovery of an oxisol subjected to four intensities of dairy cattle grazing. Soil Tillage Res. 206. https://doi.org/10.1016/j.still.2020.104813.

Koulibaly, B., Traore, O., Dakuo, D., Lalsaga, R., Lompo, F., Zombre, P., 2015. Acidification des sols ferrugineux et ferrallitiques dans les systèmes de production cotonnière au Burkina Faso. Int J Biol Chem Sci 8, 2879. https://doi.org/10.4314/ijbcs.v8i6.44.

Kumar, B., Sarkar, N.C., Maity, S., Maiti, R., 2019. Effect of different levels of Sulphur and boron on the growth and yield of sesame under red-laterite soils. Res. Crops 20, 515–524. https://doi.org/10.31830/2348-7542.2019.074.

Kumar, K.A., Swain, D.K., Bhadoria, P.B.S., 2018. Split application of organic nutrient improved productivity, nutritional quality and economics of rice-chickpea cropping system in lateritic soil. Field Crop Res. 223, 125–136. https://doi.org/10.1016/j.fcr.2018.04.007.

Lahori, A.H., Tunio, M., Ahmed, S.R., Mierzwa-Hersztek, M., Vambol, V., Afzal, A., Kausar, A., Vambol, S., Umar, A., Muhammad, A., 2024. Role of pressmud compost for reducing toxic metals availability and improving plant growth in polluted soil: challenges and recommendations. Sci. Total Environ. 951, 175493. https://doi.org/10.1016/j.scitotenv.2024.175493.

Laurent, J.Y., Brossard, M., 1991. Etude comparee de la determination du phosphore total de sols tropicaux. Cahiers - ORSsTOM, Serie Pedologie 26, 281–285.

Leão, T.P., Neves, H.V., Campos, A.F.C., Pinheiro, T.D., de Figueiredo, C.C., 2020. A conceptual model for stability and surface chemistry of oxidic soil dispersions. Colloids Surf. A Physicochem. Eng. Asp. 603, 125214. https://doi.org/10.1016/j.colsurfa.2020.125214.

Legros, J.-P., 2013. Latérites et autres sols des régions intertropicales. Bulletin 12, 369–382.

Lehto, T., 1994. Effects of soil pH and calcium on mycorrhizas of Picea abies. Plant Soil 163, 69–75. https://doi.org/10.1007/BF00033942.

Li, X., Wang, R., Lou, F., Ji, P., Wang, J., Dong, W., Tao, P., Zhang, Y., 2024. Subsoiling combine with layered nitrogen application optimizes root distribution and improve

grain **y**ield and N **e**fficiency of **s**ummer **m**aize. Agronomy 14. https://doi.org/10.3390/agronomy14061228.
Li, Y., Dong, Z.Y., Pan, D.Z., Pan, C.H., Chen, L.H., 2017. Effect of termite on soil pH and its application for termite control in Zhejiang Province, China. Sociobiology 64, 317–326. https://doi.org/10.13102/sociobiology.v64i3.1674.
de Lima, S.S., Pereira, M.G., Pereira, R.N., Pontes R.M., D.E., Rossi, C.Q., 2018. Termite mounds effects on soil properties in the **A**tlantic forest biome. Rev Bras Cienc Solo 42, 1–14. https://doi.org/10.1590/18069657rbcs20160564.
Liu, X., Liu, J., Huang, C., Liu, H., Meng, Y., Chen, H., Ma, S., Liu, Z., 2024. The impacts of irrigation methods and regimes on the water and nitrogen utilization efficiency in subsoiling wheat fields. Agric. Water Manag. 295, 108765. https://doi.org/10.1016/j.agwat.2024.108765.
Liu, X.N., Hseu, Z.Y., Chen, Z.S., 2020. Correcting the classification of plinthic Ultisols on aged alluvial terraces in Taiwan. Soil Sci. Plant Nutr. 66, 458–468. https://doi.org/10.1080/00380768.2020.1755206.
Loke, P.F., Kotzé, E., Du Preez, C.C., 2013. Impact of long-term wheat production management practices on soil acidity, phosphorus and some micronutrients in a semi-arid Plinthosol. Soil Res. 51, 415–426. https://doi.org/10.1071/SR12359.
Ma, S., Wang, C., Bi, J., Ye, F., Liu, X., 2024. Calcium carbonate enhanced **a**s uptake in Pteris vittata by increasing pH and **a**s bioavailability and mediating rhizosphere **a**s-transformation bacterial community. Environ. Exp. Bot. 226, 105949. https://doi.org/10.1016/j.envexpbot.2024.105949.
Malaisse, F., 2011. How to live and survive in Zambezian open forest (Miombo **e**coregion). Les Presses Agronomiques de Gembloux (Belgique) 23, 91–97. https://doi.org/10.5091/plecevo.2011.679.
Malik, S., Laura, J.S., Khyalia, P., 2024. Assessing the potential sustainability benefit of **a**gricultural residues: **b**iomass conversion to **b**iochar and its use for soil and crop improvement. Egypt. J. Soil Sci. 64, 1479–1493. https://doi.org/10.21608/ejss.2024.294662.1783.
Maroneze, M.M., Zepka, L.Q., Vieira, J.G., Queiroz, M.I., Jacob-Lopes, E., 2014. A tecnologia de remoção de fósforo: Gerenciamento do elemento em resíduos industriais. Revista Ambiente e Agua 9, 445–458. https://doi.org/10.4136/1980-993X.
Martins, A.P.B., Glenio, G.S., de Oliveira, V.Á., Maranhão, D.D.C., Collier, L.S., 2018. Reversibility of the hardening process of plinthite and petroplinthite in soils of the araguaia river floodplain under different treatments. Rev Bras Cienc Solo 42, 1–13. https://doi.org/10.1590/18069657rbcs20170191.
de Melo, W.J., de Melo, G.M.P., de Melo, V.P., Araujo, A.S.F., Ferraudo, A.S., Bertipaglia, L.M.A., 2020. Soil microbial biomass and enzyme activity in six Brazilian oxisols under cropland and native vegetation. Bragantia 79, 498–504. https://doi.org/10.1590/1678-4499.20200242.
Meriño-Gergichevich, C., Alberdi, M., Ivanov, A.G., Reyes-Díaz, M., 2010. Al3+-Ca2+ interaction in plants growing in acid soils: Al-phytotoxicity response to calcareous amendments. J. Soil Sci. Plant Nutr. 10, 217–243. https://doi.org/10.4067/S0718-95162010000100003.
Metahni, S., Coudert, L., Gloaguen, E., Guemiza, K., Mercier, G., Blais, J.F., 2019. Comparison of different interpolation methods and sequential Gaussian simulation to estimate volumes of soil contaminated by **a**s, Cr, **c**u, PCP and dioxins/furans. Environ. Pollut. 252, 409–419. https://doi.org/10.1016/j.envpol.2019.05.122.
de Moraes, J.M., Schuler, A.E., Dunne, T., de O. R., Figueiredo, Victoria, R.L., 2006. Water storage and runoff processes in plinthic soils under forest and pasture in **e**astern Amazonia. Hydrol. Process. https://doi.org/10.1002/hyp.6213.
Mpundu, M.M., Useni, S., Mwamba, M., Kateta, M.G., Mwansa, M., Ilunga, K., Kamenga, K.C., Kyungu, K., Nyembo, K.L., 2013. Teneurs en éléments traces métalliques dans les sols de différents jardins potagers de la ville minière de Lubumbashi et risques de contamination des cultures potagères. J. Appl. Biosci. 66, 5106–5113.
Mubemba, M.M., Sikuzani, Y.U., Kimuni, L.N., Colinet, G., 2014. Effects of carbonate and organic amendments on two vegetable crops in contaminated soil in Lubumbashi (DR Congo). Biotechnol. Agron. Soc. Environ. 18, 367–375.
Mubemba, M.M.M., Mununga, K.F., Kaumbu, K.J.-M., Mwilambwe, K.X., Maloba, K.J.-P., Banza, I.M., Mukunto, K.I., 2017. Influence des sols contaminés en cuivre sur le développement de deux variétés (locale et améliorée) de légumes dans la région de Lubumbashi (RD. Congo). J. Appl. Biosci. 115, 11410. https://doi.org/10.4314/jab.v115i1.1.
Muhirwa, F., Shen, L., Elshkaki, A., Chiaka, J.C., Zhong, S., Bönecke, E., Hirwa, H., Seka, A.M., Habiyakare, T., Tuyishimire, A., Harerimana, B., 2023. Alert in the dynamics of water-energy-food production in African countries from a nexus perspective. Resour. Conserv. Recycl. 194. https://doi.org/10.1016/j.resconrec.2023.106990.
Mujinya, B.B., Ranst, E. Van, Verdoodt, A., Baert, G., Ngongo, L.M., 2010. Termite bioturbation effects on electro-chemical properties of Ferralsols in the **u**pper Katanga (D.R. Congo). Geoderma 158, 233–241. https://doi.org/10.1016/j.geoderma.2010.04.033.
Mujinya, B.B., Mees, F., Erens, H., Dumon, M., Baert, G., Boeckx, P., Ngongo, M., Van Ranst, E., 2013. Clay composition and properties in termite mounds of the Lubumbashi area, D.R. Congo Geoderma 192, 304–315. https://doi.org/10.1016/j.geoderma.2012.08.010.
Mujinya, B.B., Adam, M., Mees, F., Bogaert, J., Vranken, I., Erens, H., Baert, G., Ngongo, M., Ranst, E. Van, 2014. Spatial patterns and morphology of termite (Macrotermes falciger) mounds in the **u**pper Katanga, D.R. Congo Catena (Amst) 114, 97–106. https://doi.org/10.1016/j.catena.2013.10.015.
Naeem, M.B., Jahan, S., Rashid, A., Shah, A.A., Raja, V., El-Sheikh, M.A., 2024. Improving maize yield and drought tolerance in field conditions through activated biochar application. Sci. Rep. 14, 1–25. https://doi.org/10.1038/s41598-024-76082-w.
Nahon, D., 2003. Altérations dans la zone tropicale. Signification à travers les mécanismes anciens et/ou encore actuels. Compt. Rendus Geosci. 335, 1109–1119. https://doi.org/10.1016/j.crte.2003.10.008.
Nascimento, D.B., do Lopes, M.L.S., Izidro, J.L.P.S., Bezerra, R.C.A., Gois, G.C., de Amaral, T.N.E., da Silva Dias, W., de Barros, M.M.L., da Silva Oliveira, A.R., de Farias Sobrinho, J.L., Coêlho, J.J., 2024. Nitrogen, phosphorus, and potassium cycling in pasture ecosystems. Ciencia Anim. Bras. 25. https://doi.org/10.1590/1809-6891v25e-76743E.
Ngon Ngon, G.F., Yongue-Fouateu, R., Bitom, D.L., Bilong, P., 2009. A geological study of clayey laterite and clayey hydromorphic material of the region of Yaoundé (Cameroon): a prerequisite for local material promotion. J. Afr. Earth Sci. 55, 69–78. https://doi.org/10.1016/j.jafrearsci.2008.12.008.
Nieminen, P., 2022. Application of **s**tandardized **r**egression **c**oefficient in meta-**a**nalysis. BioMedInformatics 2, 434–458. https://doi.org/10.3390/biomedinformatics2030028.
N'tambwe Nghonda, D. donné, Muteya, H.K., Kashiki, B.K.W.N., Sambiéni, K.R., Malaisse, F., Sikuzani, Y.U., Kalenga, W.M., Bogaert, J., 2023. Towards an **i**nclusive **a**pproach to Forest **m**anagement. In: Highlight of the Perception and Participation of Local Communities in the Management of **M**iombo Woodlands around Lubumbashi (Haut-Katanga, D.R. Congo). Forests 14. https://doi.org/10.3390/f14040687.
Obalum, S.E., Chibuike, G.U., Peth, S., Ouyang, Y., 2017. Soil organic matter as sole indicator of soil degradation. Environ. Monit. Assess. 189. https://doi.org/10.1007/s10661-017-5881-y.
O'Brien, F.J.M., Almaraz, M., Foster, M.A., Hill, A.F., Huber, D.P., King, E.K., Langford, H., Lowe, M.A., Mickan, B.S., Miller, V.S., Moore, O.W., Mathes, F., Gleeson, D., Leopold, M., 2019. Soil salinity and pH drive soil bacterial community composition and diversity along a lateritic slope in the Avon River **c**ritical **z**one **o**bservatory. Western Australia Front Microbiol 10. https://doi.org/10.3389/fmicb.2019.01486.
Ogunwole, J.O., Esu, I.E., Kparmwang, T., Chude, V.O., 2001. Effects of prolonged shaking periods and contents of iron oxides on dispersion of plinthitic soil in Nigeria. Commun. Soil Sci. Plant Anal. 32, 2293–2306. https://doi.org/10.1081/CSS-120000284.
Olego, M.Á., Quiroga, M.J., Mendaña-Cuervo, C., Cara-Jiménez, J., López, R., Garzón-Jimeno, E., 2021. Long-term effects of calcium-based liming materials on soil fertility sustainability and rye production as soil quality indicators on a typic palexerult. Processes 9. https://doi.org/10.3390/pr9071181.
Silva Martins, A.L. da, de Oliveira, A.P., de Moura, E.G., Hernan, J., 2012. Surface Infiltration on Tropical Plinthosols in Maranhão, Brazil. Water Quality, Soil and Managing Irrigation of Crops. https://doi.org/10.5772/33292.
Oluwatosin, G.A., Are, K.S., Adeyolanu, O.D., Idowu, O.J., 2020. Characteristics and agricultural potential of soils with plinthic materials in the savanna ecology of south western Nigeria. Arch. Agron. Soil Sci. 66, 1794–1811. https://doi.org/10.1080/03650340.2019.1696017.
Padonou, E.A., Djagoun, C.A.M.S., Akakpo, A.B., Ahlinvi, S., Lykke, A.M., Schmidt, M., Assogbadjo, A., Sinsin, B., 2020. Role of termites in the restoration of soils and plant richness on bowé in West Africa. Afr. J. Ecol. 58, 828–835. https://doi.org/10.1111/aje.12778.
Paul, E.A., 2016. The nature and dynamics of soil organic matter: **p**lant inputs, microbial transformations, and organic matter stabilization. Soil Biol. Biochem. 98, 109–126. https://doi.org/10.1016/j.soilbio.2016.04.001.
Pereira-De-Oliveira, L., Macedo, L., Neto, J., Santos, D., Silva, H., 2019. Viability of lateritic soil as alkaline activated precursor. MATEC Web Conf. 274, 01004. https://doi.org/10.1051/matecconf/201927401004.
Pessoa, T.N., Santos, R.S., Libardi, P.L., de Assis, I.R., Oliveira, T.S., 2024. Influence of intensive cropping of vegetables on physical and hydraulic properties and functions of an Oxisol in the Brazilian Cerrado. Catena (Amst) 235. https://doi.org/10.1016/j.catena.2023.107651.
R Core Team, 2025. A Language and Environment for Statistical Computing. R Foundation for Statistical Computing, Vienna, Austria.
Rajeev, V., Sanjeev, A., 2011. Impact of termite activity and its effect on soil composition. Tanzania J. Natl. Appl. Sci. 2, 399–404.
Ramadhan, M.N., Alfaris, M.A.A., 2023. Soil **p**roperties and **m**aize **g**rowth as **a**ffected by **s**ubsoiling and **t**raffic-**i**nduced **c**ompaction. IOP Conf. Ser. Earth Environ. Sci. 1225. https://doi.org/10.1088/1755-1315/1225/1/012077.
Ramaroson, V.H., Becquer, T., Sá, S.O., Razafimahatratra, H., Delarivière, J.L., Blavet, D., Vendrame, P.R.S., Rabeharisoa, L., Rakotondrazafy, A.F.M., 2018. Mineralogical analysis of ferralitic soils in Madagascar using NIR spectroscopy. Catena (Amst) 168, 102–109. https://doi.org/10.1016/j.catena.2017.07.016.
Roquin, C., Freyssinet, P., Zeegers, H., Tardy, Y., 1990. Element distribution patterns in laterites of southern Mali: consequence for geochemical prospecting and mineral exploration. Appl. Geochem. 5, 303–315. https://doi.org/10.1016/0883-2927(90)90006-Q.
Rosolem, C.A., Nascimento, C.A.C., Bertolino, K.M., Picoli, L.B., 2024. Humic acid enhances phosphorus transport in soil and uptake by maize. J. Plant Nutr. Soil Sci. 187, 401–414. https://doi.org/10.1002/jpln.202300413.
Rotta, L.R., Paulino, H.B., Anghinoni, I., de, Souza, E.D., Lopes, G., Carneiro, M.A.C., 2015. Phosphorus fractions and avaibility in a haplic plintthosol under no-tillage system in the brazilian Cerrado. Ciência e Agrotecnologia 39, 216–224.
le Roux, P.A.L., du Preez, C.C., Bühmann, C., 2005. Indications of ferrolysis and structure degradation in an estcourt soil and possible relationships with plinthite formation. S. Afr. J. Plant Soil 22, 199–206. https://doi.org/10.1080/02571862.2005.10634708.
Saïdou, A., Janssen, B.H., Temminghoff, E.J.M., 2003. Effects of soil properties, mulch and NPK fertilizer on maize yields and nutrient budgets on ferralitic soils in southern

Benin. Agric. Ecosyst. Environ. 100, 265–273. https://doi.org/10.1016/S0167-8809(03)00184-1.
Sanchez, P.A., 2018. Properties and Management of Soils in the Tropics. John Wiley & Sons ed New York. https://doi.org/10.1017/CBO9781107415324.004.
Santos, T.E.D., Gomes, F.H., Mancini, M., Nóbrega, G.N., Avanzi, J.C., Marques, J.J., Souza Júnior, V.S. de, Inda, A.V., Silva, M.L.N., Curi, N., 2023. Detailed characterization of plinthic soils in southern Mali, sub-Saharan Africa, as a secure basis for specific soil management and food security. Catena (Amst) 226. https://doi.org/10.1016/j.catena.2023.107088.
Sapkota, T.B., Jat, M.L., Jat, R.K., Kapoor, P., Stirling, C., 2016. Yield estimation of food and non-food crops in smallholder production systems, methods for measuring greenhouse gas balances and evaluating mitigation options in smallholder. Agriculture. https://doi.org/10.1007/978-3-319-29794-1_8.
Šarauskis, E., Sokas, S., Rukaitė, J., 2024. Variable depth tillage: importance, applicability, and impact—an overview. AgriEngineering 6, 1870–1885. https://doi.org/10.3390/agriengineering6020109.
Sarkar, A., Bandyopadhyay, P.K., 2018. Effect of incubation duration of incorporated organics on saturated hydraulic conductivity, aggregate stability and sorptivity of alluvial and red-laterite soils. J. Indian Soc. Soil Sci. 66, 370–380. https://doi.org/10.5958/0974-0228.2018.00046.4.
Sediqui, N., Amin, M.W., Dawlatzai, N., Gulab, G., Poyesh, D.S., Terada, N., Sanada, A., Kamata, A., Koshio, K., 2024. Elucidation of shoot and root growth, physiological responses, and quality traits of tomato (Solanum lycopersicon L.) exposed to elevated calcium carbonate concentrations. Horticulturae 10. https://doi.org/10.3390/horticulturae10060573.
Seymour, C.L., Milewski, A.V., Mills, A.J., Joseph, G.S., Cumming, G.S., Cumming, D.H. M., Mahlangu, Z., 2014. Soil Biology & Biochemistry do the large termite mounds of Macrotermes concentrate micronutrients in addition to macronutrients in nutrient-poor African savannas? Soil Biol. Biochem. 68, 95–105. https://doi.org/10.1016/j.soilbio.2013.09.022.
Shi, J., Li, J., Pan, Y., Zhao, M., Zhang, R., Xue, Y., Liu, Y., 2024. The physiological response mechanism of Peanut leaves under Al stress. Plants 13. https://doi.org/10.3390/plants13121606.
da Silva, A.P.V., Silva, A.O., de Lima, F.R.D., Benedet, L., Carriço, C.O., de J. A., Franco, Guilherme, L.R.G., Carneiro, M.A.C., 2024. Reduction of pH on the bioavailability of potentially toxic elements for plants grown in Iron mining tailing. Water Air Soil Pollut. 235, 1–16. https://doi.org/10.1007/s11270-024-07205-2.
Smith, J., Smith, P., 2007. Environmental Modeling: An Introduction. Oxford University Press, Oxford, UK.
Soil Survey Staff, 2014. Keys to soil taxonomy. In: Soil Conservation Service, 12th ed. USDA-NRCS, Washington DC.
Steppuhn, H., Waddington, J., McConkey, B.G., 1995. Subsoiling to improve snowmelt infiltration and alfalfa yields within tall wheatgrass windbreaks. Can. Agric. Eng. 37, 261–268.
Stiles, C.A., Mora, C.I., Driese, S.G., 2001. Pedogenic iron-manganese nodules in Vertisols: a new proxy for paleoprecipitation? Geology 29, 943–946. https://doi.org/10.1130/0091-7613(2001)029<0943:PIMNIV>2.0.CO;2.
Stupen, R., Ryzhok, Z., Stupen, N., Stupen, O., Dudych, H., 2022. Methods of building a digital relief model using the application of geoinformation. In: 2022 International Conference of Young Professionals, GeoTerrace 2022. https://doi.org/10.3997/2214-4609.2022590013.
Tandzi, L.N., Mutengwa, C.S., 2020. Estimation of maize (Zea mays L.) yield per harvest area: appropriate methods. Agronomy 10, 1–18. https://doi.org/10.3390/agronomy10010029.
Tsamos, P., Stefanou, S., Noli, F., 2024. Assessment of distribution of heavy metals and radionuclides in soil and plants nearby an oil refinery in northern Greece. Case Stud. Chem. Environ. Eng. 9, 100593. https://doi.org/10.1016/j.cscee.2023.100593.
Tshibangu, K. Azadi A., Lwalaba, Wa L.J., Kirika, A.B., Mavungu, M.J., Manda, K.G., Iband, K.M., Baert, G., Haesaert, G., Mukobo, M.R.P., 2022. Effect of phosphorus and arbuscular mycorrhizal Fungi (AMF) inoculation on growth and productivity of maize (Zea mays L.) in a tropical Ferralsol. Gesunde Pflanzen 74, 159–165. https://doi.org/10.1007/s10343-021-00598-8.
Useni, S.Y., Ilunga, G.M., Mulembo, T.M., Ntumba, B., Longanza, L.B., 2014. Amélioration de la qualité des sols acides de Lubumbashi (Katanga, RD Congo) par l ' application de différents niveaux de compost de fumiers de poules. J. Appl. Biosci. 77, 6523–6533.
Useni, S.Y., Malaisse, F., Dibwe, D., Mwembu, D., Bogaert, J., 2024. Lubumbashi (DR Congo): navigating the socio-ecological complexities of a vital mining hub. Cities 154, 105341. https://doi.org/10.1016/j.cities.2024.105341.
Venables, W.N., Ripley, B.D., 2002. Modern Applied Statistics with S-Plus, 4th ed. Springer-Verlag, New York, NY.
Voltr, V., Menšík, L., Hlisnikovský, L., Hruška, M., Pokorný, E., Pospíšilová, L., 2021. The soil organic matter in connection with soil properties and soil inputs. Agronomy 11. https://doi.org/10.3390/agronomy11040779.
Walkley, A., Black, I.A., 1934. An examination of the degtjareff method for determining soil organic matter, and a proposed modification of the chromic acid titration method. Soil Sci. 37, 29–38. https://doi.org/10.1097/00010694-193401000-00003.
Wang, L., Yu, X., Gao, J., Ma, D., He, T., Hu, S., 2024a. Effect of subsoiling on the nutritional quality of grains of maize hybrids of different eras. Plants 13, 1900. https://doi.org/10.3390/plants13141900.
Wang, S., Liu, Z., Obalum, S.E., Liang, C., Han, K., Han, H., 2023b. Effects of subsoiling depth on soil aggregate stability and carbon storage in a clay-loam soil. J. Soil Sci. Plant Nutr. 23, 3302–3312. https://doi.org/10.1007/s42729-023-01246-y.
Wang, X., Geng, L., Zhou, H., Huang, Y., Ji, J., 2023a. Effects of subsoiling with different wing Mounting Heights on soil water infiltration using HYDRUS-2D simulations. Agronomy 13. https://doi.org/10.3390/agronomy13112742.
Wang, X., Du, R., Geng, L., Zhou, H., Ji, J., 2024b. Performance evaluation of a Cicada-inspired subsoiling tool using DEM simulations. Biomimetics 9. https://doi.org/10.3390/biomimetics9010025.
Wang, Y., Wu, T., Huang, J., Tian, P., Zhang, H., Yang, T., 2020. Soil hydraulic properties of plinthosol in the middle Yangtze River basin. Southern China Water (Switzerland) 12. https://doi.org/10.3390/w12061783.
Wang, Y., Wang, C., Zhang, C., Liao, Q., Feng, Z., Zou, X., 2024c. Variations in provenance and transport of terrestrial organic matter in the Changjiang River during the flood season. Catena (Amst) 242, 108083. https://doi.org/10.1016/j.catena.2024.108083.
Widdowson, M., 2009. Evolution of Laterite in Goa, Natural Resources of Goa: A Geological Perspective.
Wildemeersch, J.C.J., Garba, M., Sabiou, M., Sleutel, S., Cornelis, W., 2015. The effect of water and soil conservation (WSC) on the soil chemical, biological, and physical quality of a Plinthosol in Niger. Land Degrad. Dev. 26, 773–783. https://doi.org/10.1002/ldr.2416.
Woś, B., Likus-Cieślik, J., Pająk, M., Pietrzykowski, M., 2024. How tree species have modified the potentially toxic elements distributed in the developed soil–plant system in a post-fire site in highly industrialized region. Environ. Monit. Assess. 196. https://doi.org/10.1007/s10661-024-12933-3.
WRB, I.W.G., 2022. World Reference Base for soil resources. International soil classification system for naming soils and creating legends for soil maps. In: International Union of Soil Sciences (IUSS), Vienna, Austria, 4th ed.
WRB-IUSS, 2007. World Reference Base for soil resources 2006, first update 2007. World Soil Res. Rep. No 103, 128.
WRB-IUSS, 2015. World Reference Base for Soil Resources 2014, update 2015 International soil classification system for naming soils and creating legends for soil maps. In: World Soil Resources Reports No. 106. Rome.
Wu, J., Wang, R., Zhao, W., Zhao, K., Wu, S., Zhang, J., Wang, H., Fu, G., Huang, M., Li, Y., 2024. Combined subsoiling and ridge-furrow rainfall harvesting during the summer fallow season improves wheat yield, water and nutrient use efficiency, and quality and reduces soil nitrate-N residue in the dryland summer fallow-winter wheat rotation. Front. Plant Sci. 15, 1–14. https://doi.org/10.3389/fpls.2024.1401287.
Wu, S.F., Wu, P.T., Feng, H., Bu, C.F., 2010. Influence of amendments on soil structure and soil loss under simulated rainfall China's loess plateau. Afr. J. Biotechnol. 9, 6116–6121. https://doi.org/10.4314/ajb.v9i37.
Xie, G., Liang, M., Chen, P., Zhang, C., Fan, M., Wang, C., Zhao, L., 2024. The effects of tillage and the combined application of organic and inorganic fertilizers on the antioxidant enzyme activity and yield of maize leaves. Agronomy 14. https://doi.org/10.3390/agronomy14050968.
Xu, F.Q., Meng, L.L., Kuča, K., Wu, Q.S., 2024. The mechanism of arbuscular mycorrhizal fungi-alleviated manganese toxicity in plants: a review. Plant Physiol. Biochem. 213. https://doi.org/10.1016/j.plaphy.2024.108808.
Yaro, D.T., Kparmwang, T., Raji, B.A., Chude, V.O., 2006. The extent and properties of Plinthite in a landscape at Zaria, Nigeria. Int. J. Soil Sci. 1, 171–183.
Yaro, D.T., Kparmwang, T., Raji, B.A., Chude, V.O., 2008. Extractable micronutrients status of soils in a plinthitic landscape at Zaria, Nigeria. Commun. Soil Sci. Plant Anal. 39, 2484–2499. https://doi.org/10.1080/00103620802292913.
Yoboue, K.E., Kouakou, C.H., Akotto, O.F., Yao-Kouame, A., 2019. Etude des variations des teneurs de quelques oxydes de deux types de sols à plinthites observés à Yébouékro (Djékanou) dans le centre-sud de la Côte d'Ivoire. Int J Biol Chem Sci 13, 1180. https://doi.org/10.4314/ijbcs.v13i2.46.
Yruela, I., 2009. Copper in plants: acquisition, transport and interactions. Funct. Plant Biol. 36, 409–430. https://doi.org/10.1071/FP08288.
Zhang, Y., Ju, S., Wang, W., Wu, F., Pan, K., 2024. Effects of decomposed and undecomposed straw of three crops on clubroot disease of Chinese cabbage and soil nutrients. Sci. Rep. 14, 22990. https://doi.org/10.1038/s41598-024-72899-7.